RSC Advances

ROYAL SOCIETY OF CHEMISTRY

www.rsc.org/advances

Mononuclear Zn(II) and Cu(II) Complexes with a Simple Diamine Ligand: Synthesis, Structure, Phosphodiester Binding and DNA Cleavage Studies

Popuri Sureshbabu[a] , A.A.J. Sudarga Tjakraatmadja[b] , Chittepu Hanmandlu[a] , K. Elavarasan[a], Nora Kulak [b,]* and Shahulhameed Sabiah[a,] *

[a]Department of Chemistry, Pondicherry University, Pondicherry- 605 014, India.

[b]Institute of Chemistry and Biochemistry, Freie Universtität Berlin, Germany.

Abstract

Two mononuclear complexes, $[Cu(dach)_2(ClO_4)_2]$ **1a** and $[Zn(dach)_2](ClO_4)_2$ **2a**, with simple 1,2-diaminocyclohexane (dach) ligands were synthesized and characterized by elemental analysis, UV-Vis, EPR and IR spectroscopy. The single crystal XRD of **1a** and **2a** shows that the metal ion has octahedral and tetrahedral geometry, respectively. Both complexes bind with phosphodiesters such as BNPP (bis(*p*-nitrophenyl)phosphate) and DPP (diphenylphosphate) and their binding affinity was studied by electronic absorption spectroscopy. Complex **1a** binds with DPP with K_b= 23 M^{-1} and **2a** shows K_b= 1.15× 10^3 M^{-1}. Both complexes interact with BNPP to result in $[Cu(dach)_2(BNPP)_2]$ **3**, $[Zn(dach)_2(BNPP)_2]$ **4**, respectively. These phosphate adducts were well characterized by different spectroscopic techniques and single crystal XRD. The X-ray structures confirm that complexes **3** and **4** are mononuclear with Cu(II) and Zn(II) in octahedral geometry provided by two bidentate dach ligands and two monodentate O donors from BNPP moieties. The nuclease activity of **1a** and **2a** with supercoiled plasmid DNA pBR322 was examined by gel electrophoresis, which reveals that complex **1a** exhibits a significant DNA cleavage activity via oxidative mechanism whereas the corresponding complex **2a** did not cleave the DNA. To understand the stereo chemical influence of the dach ligand on DNA cleavage activity, copper and zinc complexes derived from enantiopure form of dach namely [Cu((*R*,*R*)-

trans-dach)$_2$(ClO$_4$)$_2$] **1b**, [Cu((*S*,*S*)-*trans*-dach)$_2$(ClO$_4$)$_2$] **1c** & [Cu(*cis*-dach)$_2$(ClO$_4$)$_2$] **1d** and [Zn((*R*,*R*)-*trans*-dach)$_2$](ClO$_4$)$_2$ **2b**, [Zn((*S*,*S*)-*trans*-dach)$_2$](ClO$_4$)$_2$ **2c** & [Zn(*cis*-dach)$_2$](ClO$_4$)$_2$ **2d** were also investigated. All the Cu(II) complexes oxidatively cleave pBR322 at 25 uM, out of which complex **1b** is remarkable to cleave up to 20% Form II and 80% Form III. The binding affinity of these complexes with CT-DNA (Calf thymus-DNA) was studied by electronic absorption spectroscopy and showed moderate to strong K_b values. Electrochemical analyses, viscosity measurements and circular dichroism (CD) studies were carriedout to understand the mode of binding with CT-DNA. The shift in ΔEp, $E_{1/2}$ and Ipc values suggest that there is a minor groove interaction existing between CT-DNA and copper complexes. The groove binding is further supported by viscosity measurements and CD spectra.

Key words: 1,2-diaminocyclohexane, dach, mononuclear copper, Phosphodiesters, BNPP, DPP, DNA cleavage.

1. Introduction

Mononuclear transition metal complexes are found to catalytically hydrolyze biomolecules such as DNA and RNA and have been studied for almost 30 years.[1-4] Since DNA and RNA contain phosphodiester bonds, binding, hydrolytic and oxidative cleavage of them play a significant role in gene-targeted cancer therapy.[5, 6] However, the phosphodiester bonds of DNA are known to be very stable under physiological conditions and the half-life of DNA hydrolysis in the absence of metal is estimated to be about 200 million years.[7] Therefore, DNA cleavage by artificial nucleases under physiological conditions is a challenging topic. The DNA cleavage mechanism is preceded either oxidatively or hydrolytically and is dependent on the central metal atom and the ligand.[8, 9] The hydrolytic cleavage mechanism is preferred by redox-inactive metals like zinc, magnesium and zirconium, whereas the oxidative cleavage mechanism is preferred by

redox-active metals such as iron and copper. Several mononuclear Cu(II) and Zn(II) complexes have been the subject of intense investigation for DNA binding and cleavage studies. [10-14] Cu(II) was found to cleave oxidatively with higher affinity than any other divalent transition metal. [15-16]

Our goal was to investigate the phosphodiester binding and DNA cleavage activity of Cu(II) and Zn(II) complexes with a simple 1,2-diaminocyclohexane (dach) bidentate ligand. The ligand is chiral whose platinum analog oxaliplatin gained numerous attention.[17a,b] In this connection, the literature also supports the importance of N-donor ligands and their metal complexes as anticancer, antimicrobial and antibiofilm agents apart from their catalytic activity in organic transformations.[17] However, this simple ligand has not been employed for phosphodiester binding and DNA cleavage studies especially with homoleptic mononuclear copper and zinc complexes. Hence, we have synthesized mononuclear copper (**1a**-**1d**) and zinc (**2a**-**2d**) complexes and examined their phosphodiester binding, DNA cleavage studies, Electrochemical analyses, viscosity measurements and circular dichroism (CD) studies apart from routine spectral studies. An important observation from the current study is the efficient oxidative DNA cleavage activity of complex **1b** and strong phosphodiester binding affinity of complex **2a**.

2. Results and Discussion

2.1. The ligand and its complexes

1,2-diaminocyclohexane (dach) is a simple bidentate ligand which is available in *cis*, *trans* (*R*,*R*/*S*,*S*) or mixture of *cis*/*trans* forms. The complexation of racemic dach with metal salts, $Cu(ClO_4)_2.6H_2O$ and $Zn(ClO_4)_2.6H_2O$ in a 2:1 ratio achieved the desired complexes **1a** and **2a** in good yields as depicted in scheme 1. In order to obtain the enantiopure dach ligand, commercially available *cis/trans*-dach was treated with L-(+) or D-(+)-Tartaric acid as reported

in literature.[18] Their corresponding copper (**1b-1d**) and zinc (**2b-2d**) complexes were synthesized similar to scheme 1. The complexes were characterized by elemental analysis, UV-Vis, IR, ESI-MS, EPR (in case of **1a**), ^{1}H NMR and ^{13}C NMR spectra (in case of **2a**).

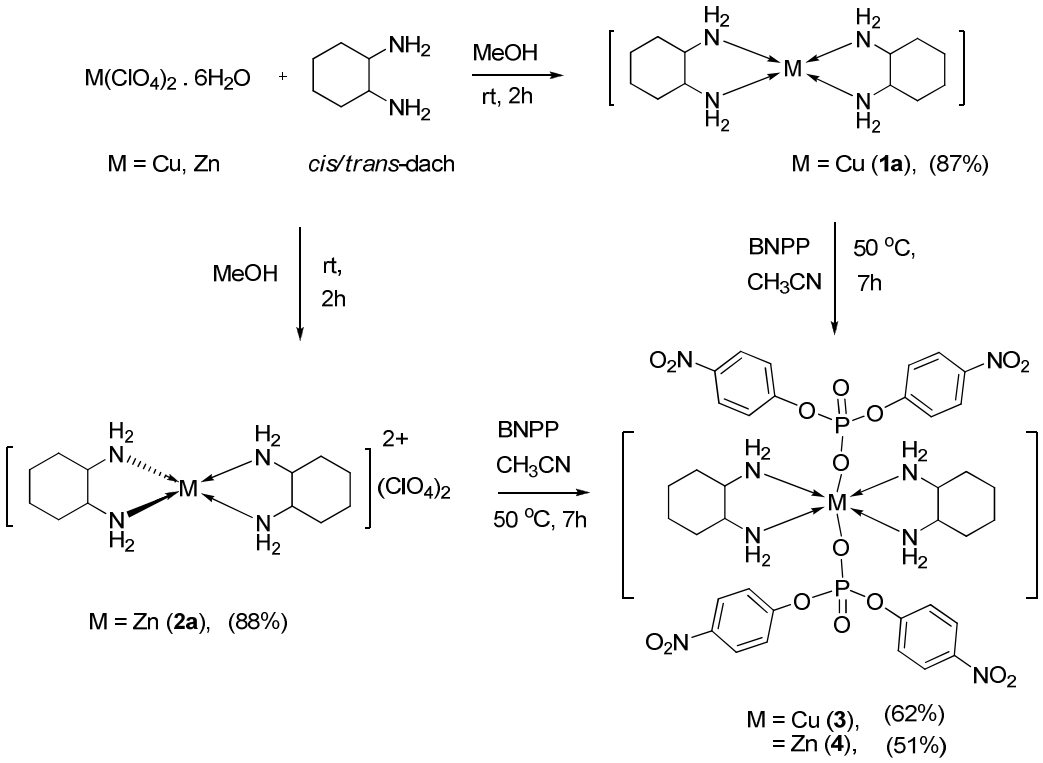

Scheme 1. Synthesis of metal complexes **1a**, **2a**, **3** and **4**.

The reaction of $[Cu(dach)_2(ClO_4)_2]$ **1a** and $[Zn(dach)_2](ClO_4)_2$ **2a** with BNPP in a 1:2 ratio resulted in phosphodiester-bound complexes $[Cu(dach)_2(BNPP)_2]$ **3** and $[Zn(dach)_2(BNPP)_2]$ **4** in moderate yield, respectively. These complexes are neutral and characterized by routine spectroscopic techniques. They are air stable and soluble in common organic solvents (**1a** and **2a** are soluble in water, acetonitrile and DMSO; **3** is soluble in acetonitrile/water mixture, DMSO and **4** is soluble in methanol, ethanol and DMSO).

2.2. Crystal Structures of 2a, **3** and **4**

Complexes **2a**, **3** and **4** are structurally characterized by X-ray crystallography (Fig. 1), whereas the crystal structure of the Cu(II) complex **1a** has already been reported.[19a] However,

the synthetic procedure of complex **1a** and the method of getting single crystals in the present study are different from literature procedure (Refer: Experimental section). Single crystals of complex **2a** were obtained from methanol as colorless needles. Complexes **3** & **4** are crystallized from the mixture of acetonitrile/water (1:1 v/v) as purple and pale yellow crystals. The crystallographic details of **2a**, **3** and **4** are summarized in Table 1. The crystal structures of **2a**, **3** and **4** with the atom labelling scheme are shown in Fig. 1. Selected bond lengths and bond angles around the metal center are provided in Table 2. In the above structures *trans* form of dach ligands are coordinated to the metal.

The asymmetric unit in complex **2a** is composed of one molecule, with in the molecule inversion centre is present. It consists of $[Zn(dach)_2]^{2+}$ and two perchlorate ions. The Zn(II) ion in the complex **2a** possesses tetrahedral geometry. The coordination is provided by two bidentate amine nitrogens from dach ligands. There is no interaction with perchlorate ions to the metal. The average Zn-N bond distance 2.017 Å (Table 1) is an agreement with the values reported for other Zn(II) diamine complexes.[20] Several hydrogen bonds between the hydrogen atoms on N(3), and the perchlorate oxygens stabilize the structure. In addition, two molecules are linked by a moderate hydrogen bonding interaction through the hydrogen on N(3) and O(1) with an N(3)-H···O(1) bond length of 2.727 Å and bond angle of ∠N(3)-H-O(1) = 161.27°. The crystal packing in this complex appears as two dimensional sheets like structure with perchlorates placed between them via O···H-N interactions (Fig. 2a).

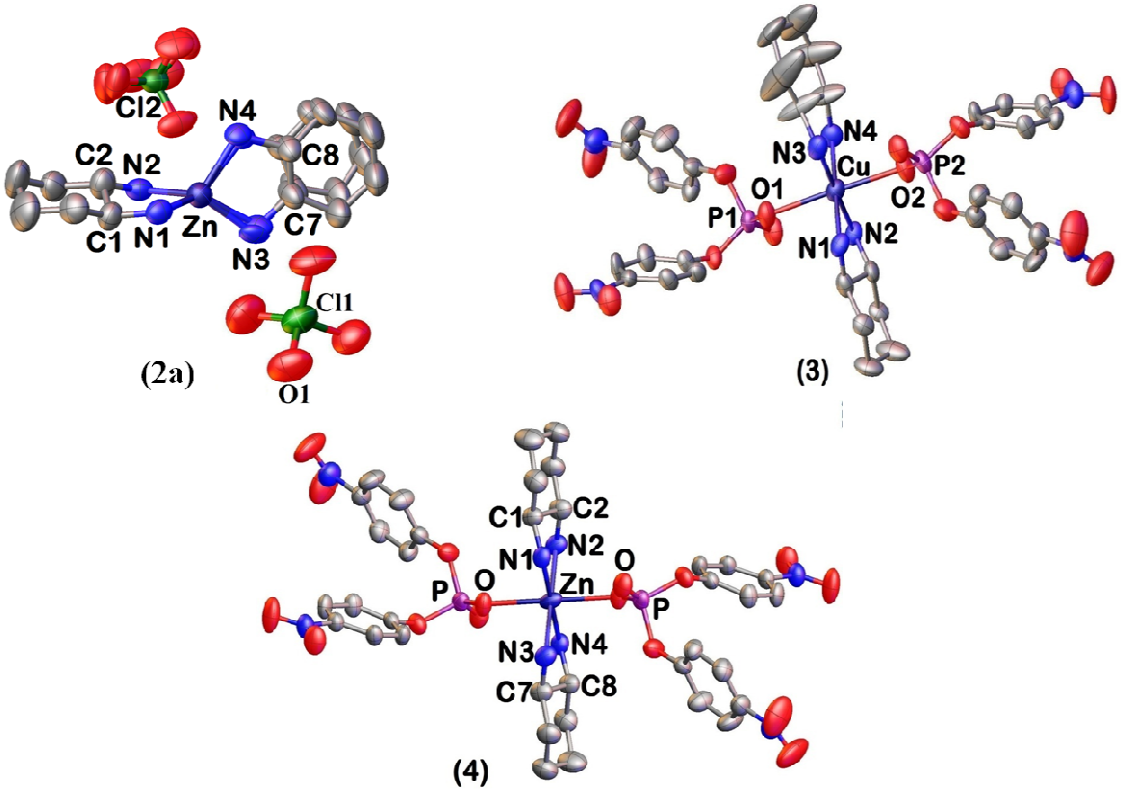

Fig. 1. Crystal structures of **2a**, **3** and **4** with the atom numbering scheme (30% probability thermal ellipsoids). Hydrogen atoms are omitted for clarity. The N3, N4 and C7-C12 atoms of ligands and perchlorate ion are disordered.

The asymmetric unit in complexes **3** and **4** is composed of one independent molecules and inversion center is present with in the molecule. These complexes are mononuclear neutral molecules with Cu(II) and Zn(II) in O_h geometry. The coordination is provided by two bidentate amine nitrogens from the dach ligand and two monodentate oxygens from the BNPP moieties. The amine nitrogen binds the metal along the equatorial plane and BNPP binds the metal along the axial plane. The average Cu-N, Zn-N bond distances of 2.011 Å and 2.108 Å (Table 1) are in agreement with the values reported for other Cu(II), Zn(II) diamine complexes.[19-21] The average Zn-N bond length in **4** is slightly increased due to the strong coordination of BNPP to the metal ion. The complex **3** contains moderately strong O···H-N hydrogen bond interactions, which are

formed between the oxygen of BNPP with the hydrogen of the amines in the range 2.071-2.613 Å, with a bond angle of 150.58°. The complex **4** contains moderate intermolecular hydrogen bonds between the hydrogens on N(2) (amine), the oxygen of BNPP O(4) [bond length N(3)-H···O(1) = 2.147 Å, bond angle ∠N(3)-H···O(1) = 145°] and hydrogens on C(cyclohexyl), the oxygen of NO_2 from BNPP [C(5)-H···O(6) = 2.538 Å, bond angle ∠C(5)-H···O(6) = 150.90°] which all stabilize the structure. The crystal packing in **3** and **4** are two dimensional sheets like structure (Fig. 2b and 2c).

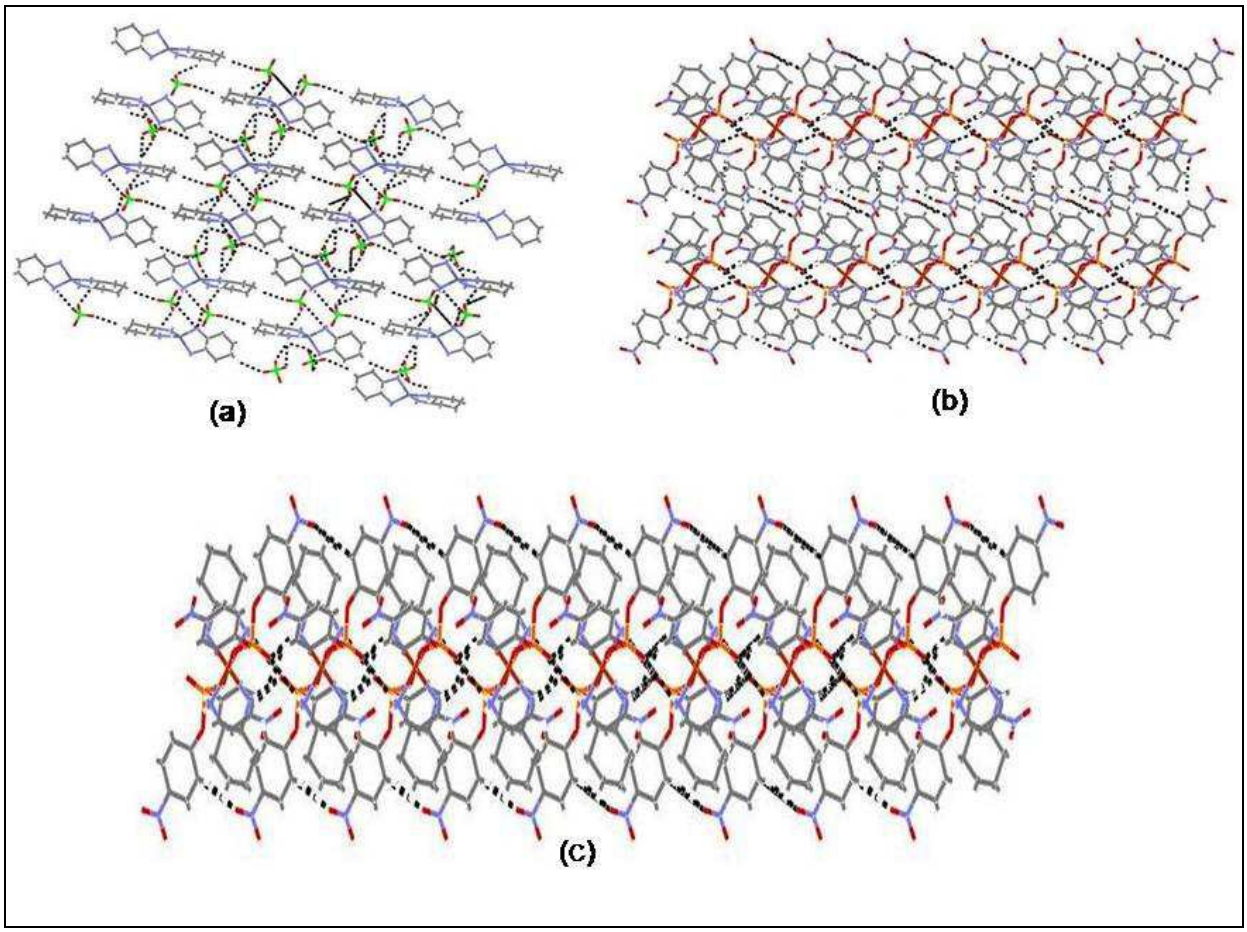

Fig. 2. Illustration of the crystal packing in complexes (a) $[Zn(dach)_2](ClO_4)_2$ **2a**, (b) $[Cu(dach)_2(BNPP)_2]$ **3** and (c) $[Zn(dach)_2(BNPP)_2]$ **4**.

Table 1

Crystallographic data for the complexes **2a**, **3** and **4**

Parameters	**2a**	**3**	**4**
CCDC No	868977	868978	869026
Molecular formula	$C_{12}H_{28}Cl_2ZnN_4O_8$	$C_{36}H_{44}CuN_8O_{16}P_2$	$C_{36}H_{44}ZnN_8O_{16}P_2$
Molecular weight	492.65	970.28	972.12
Crystal system	Triclinic	Triclinic	Triclinic
Space group, Z	$P\bar{1}$, 2	$P\bar{1}$, 1	$P\bar{1}$, 1
a (Å)	7.1131(3)	6.4876(10)	6.5343(3)
b (Å)	12.3658(8)	12.2250(2)	12.3708(6)
c (Å)	12.6629(8)	13.3630(2)	13.0811(7)
α (^{0})	111.010(6)	91.909(13)	93.630(4)
β (^{0})	95.419(5)	98.916(13)	97.837(4)
γ (^{0})	94.912(5)	92.458(13)	91.708(4)
V (Å^3)	1026.53(10)	1045.2(3)	1044.64(9)
Temperature (K)	293	298	298
λ (Å)	0.7107	0.7107	0.7107
D_c (mg/m^3)	1.594	1.541	1.542
Reflections collected	9666	7629	9666
Reflections used	5528	4589	5598
F(000)	512	500	503
abs. coeff.,μ (cm^{-1})	1.502	0.861	0.681
No.of refined parameters	354	568	286
R^a[1>2σ(I)]	0.1281	0.0708	0.0588
Rw^b	0.1342	0.1758	0.1165
Goodness –of–fit	0.939	1.025	1.032

Table 2

Selected bond distances (Å) and bond angles (°) of $[Zn(dach)_2](ClO_4)_2$ **2a**, $[Cu(dach)_2(BNPP)_2]$ **3** and $[Zn(dach)_2(BNPP)_2]$ **4**

Complex **2a**		Complex **3**		Complex **4**	
Bond length	(Å)				
Zn-N1	2.044	Cu-N1	2.033	Zn-N1	2.067
Zn-N2	2.001	Cu-N2	1.983	Zn-N2	2.149
Zn-N3	1.998	Cu-N3	2.006	Zn-N3	2.067
Zn-N4	2.026	Cu-N4	2.024	Zn-N4	2.149
		Cu-O1	2.478	Zn-O1	2.280
		Cu-O2	2.484	Zn-O2	2.280
Bond angle	(°)				
N1-Zn-N2	85.99	N1-Cu-N2	85.08	N1-Zn-N2	82.08
N1-Zn-N3	122.42	N1-Cu-N3	96.27	N1-Zn-N3	97.93
N1-Zn-N4	113.85	N1-Cu-N4	178.58	N1-Zn-N4	180.00
N2-Zn-N3	126.93	N3-Cu-N2	84.52	N3-Zn-N4	82.08
N2-Zn-N4	123.91	N3-Cu-N4	178.42	N3-Zn-N2	180.00
N3-Zn-N4	87.19	O1-Cu-N1	93.56	O1-Zn-N1	90.51
		O1-Cu-N2	92.54	O1-Zn-N2	91.97
		O1-Cu-N3	88.18	O1-Zn-N3	89.49
		O1-Cu-N4	87.64	O1-Zn-N4	88.03

3. Spectral Characterization

All the Copper (**1a**-**1d**) and Zinc (**2a**-**2d**) complexes were characterized by analytical and spectroscopic techniques. As representative examples **1a** & **2a** were chosen along with **3** and **4**.

3.1. UV-Vis spectra

The UV-Vis spectra of complexes **1a**, **2a**, **3** and **4** at room temperature were measured in the range 190-1100 nm and are shown in Fig. 3. The absorption spectra of **1a** in acetonitrile and **3** in acetonitrile/water (1:1 v/v ratio) displayed a d-d transition at 546 nm (ε = 92 M^{-1} cm^{-1}) and 548 nm (ε = 58.2 M^{-1} cm^{-1}), respectively. These transitions are may be due to $^2B_{1g} \rightarrow {}^2E_g$

transition of tetragonally distorted Cu(II) in octahedral geometry.[22-26] The dach ligand shows weak ligand centered transitions at 290 nm (ε = 0.5 M^{-1} $cm^{-}1$). The absorption spectrum of complex **2a** in acetonitrile displayed ligand centered transitions at 276 nm (ε = 16.4 M^{-1} cm^{-1}), whose molar extinction coefficient is comparable with free dach ligand [λ = 290 nm; ε = 0.5 M^{-1} cm^{-1}]. Complex **4** in methanol shows an intense absorption at 285 nm (ε = 4.06 x10^4 M^{-1} cm^{-1}), due to BNPP to Cu(II) LMCT transition. The UV-Vis spectra of complexes **1b-1d** & **2b-2d** are identical to that of complexes **1a** & **2a** respectively.

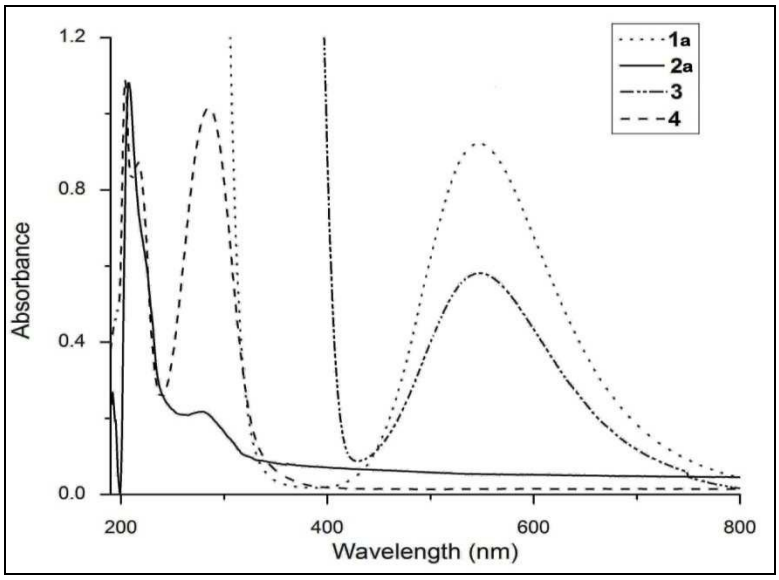

Fig. 3. Electronic absorption spectra of complexes **1a**, **2a**, **3** and **4** in different solvents {**1a**, **2a** in acetonitrile, **3** in acetonitrile/water (1:1 v/v) and **4** in methanol}.

3.2. Infrared spectra

The IR spectra of complexes **1a**, **2a**, **3** and **4** were recorded in the region 4000-400 cm^{-1} at room temperature. All Complexes exhibit characteristic broad envelope at 3246-3369 cm^{-1} attributed to $\nu_{(NH2)}$ coordinated to Cu and Zn centers.[14, 27] The sharp bands at 2854-2949 cm^{-1}, are due to $\nu_{(CH2)}$ vibrations of the cyclohexyl ring. For complex **1a** a broad intense band at 1088 cm^{-1} and a weak band at 940 cm^{-1} are observed which reveals that the perchlorate ion is

coordinated to the metal. The X-ray structure of **1a**,[19a] where perchlorates are coordinated to metal center supports this observation. For complex **2a**, a broad intense band appeared at 1150 cm^{-1} attributed to triply degenerate asymmetric stretching mode of the Td perchlorate anion, which clearly indicates that the perchlorate ion is not in the coordination sphere.[19a, 28] Apart from this, a sharp band at 628 cm^{-1}, due to triply degenerate asymmetric bending mode of the perchlorate anion is observed in **1a** and **2a**. Complexes **3** and **4** displayed aromatic $\nu_{C=C}$ bands in the region 1588-1592 cm^{-1} and $\nu_{(P=O)}$ bands in the region 1257-1265 cm^{-1}, as well as $\nu_{(P-O)}$ bands in the region 1024- 907 cm^{-1} due to BNPP moieties.

3.3. EPR studies

The solution EPR spectra of Cu(II) complexes **1a** and **3** were recorded with a magnetic field strength of 2000-4500 G (Fig. 4 and 5). The EPR spectrum of complex **1a** revealed an isotropic behavior with a broad signal indicating that the Cu(II) ion displays an octahedral geometry with $g_{iso} = 2.071$. Whereas at LNT shows $g_{\|} = 2.15$ with distorted octahedral geometry.

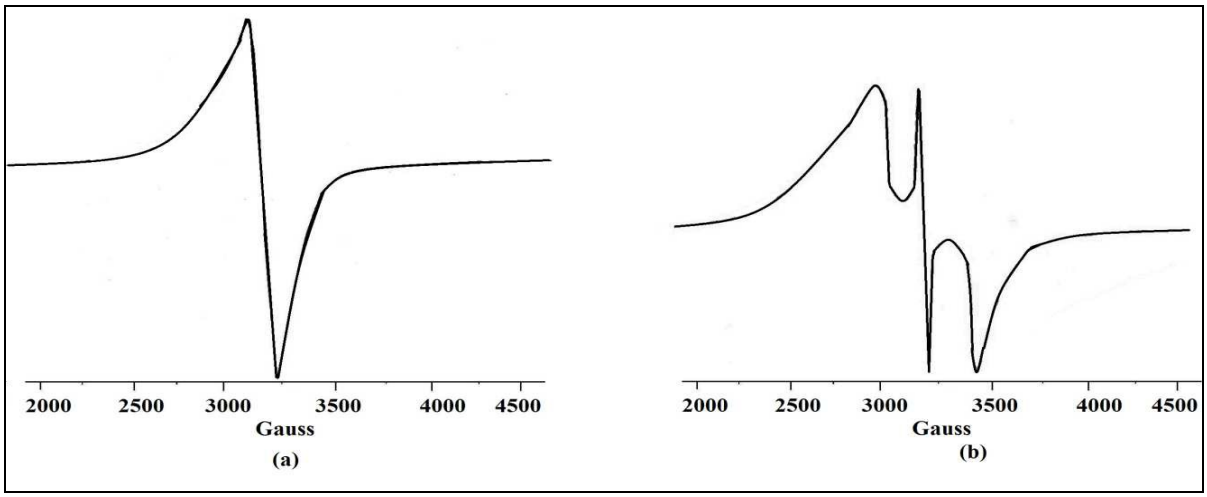

Fig. 4. EPR spectrum of $[Cu(dach)_2(ClO_4)_2]$, **1a** at (a) RT and (b) LNT, scan range = 2000–4500 G, microwave frequency = 9.40715 GHz, mod. amplitude = 5 G.

The EPR spectrum of complex **3** revealed two signals at room temperature with $g_{\|}$ = 2.404 and $g_{\perp} = 2.071$ and at LNT $g_{\|} = 2.186$, $g_{\perp} = 2.06$; $A_1 = 180$ G respectively indicating that

the Cu(II) ion is in severe distorted octahedral geometry. The obtained $g_{\|}$ and $g_{\perp}$ values are comparable with literature reports.[29-33]

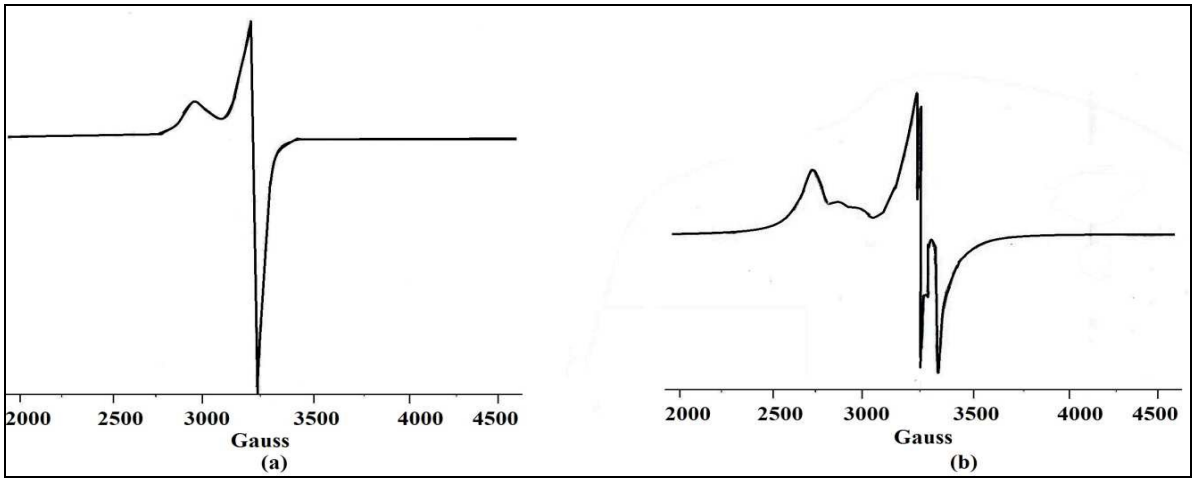

Fig. 5. EPR spectrum of $[Cu(dach)_2(BNPP)_2]$ **3** at (a) RT and (b) LNT, scan range = 2000–4500 G, microwave frequency = 9.40689 GHz, mod. amplitude = 5 G.

4. Binding and Cleavage Studies

4.1. Phosphodiester Binding studies by Electronic Absorption Spectroscopy

The binding affinity of phosphodiesters with complexes **1a** and **2a** was studied by electronic absorption spectroscopy. Since diphenylphosphate (DPP) is stable towards hydrolysis, it was chosen for binding studies. In the absence of DPP, complex **1a** shows a d-d transition at λ_{max}= 546 nm (ε = 92 M^{-1} cm^{-1}) and **2a** shows a ligand centered transition band at λ_{max}= 276 nm (ε = 16.4 M^{-1} cm^{-1}). To an acetonitrile solution of **1a** were added aliquots of DPP through a micro-litre syringe. After each addition, the solution was stirred for 1 minute and the visible spectrum was recorded (Fig. 6a). The color of the solution changed from purple to light yellow and the absorbance of λ_{max}= 546 nm decreased after every addition. A new band with λ_{max}= 660 nm (ε = 69.5 M^{-1} cm^{-1}) was observed which is postulated to be a DPP bound Cu(II) complex with an isobestic point of λ_{max} = 630 nm.

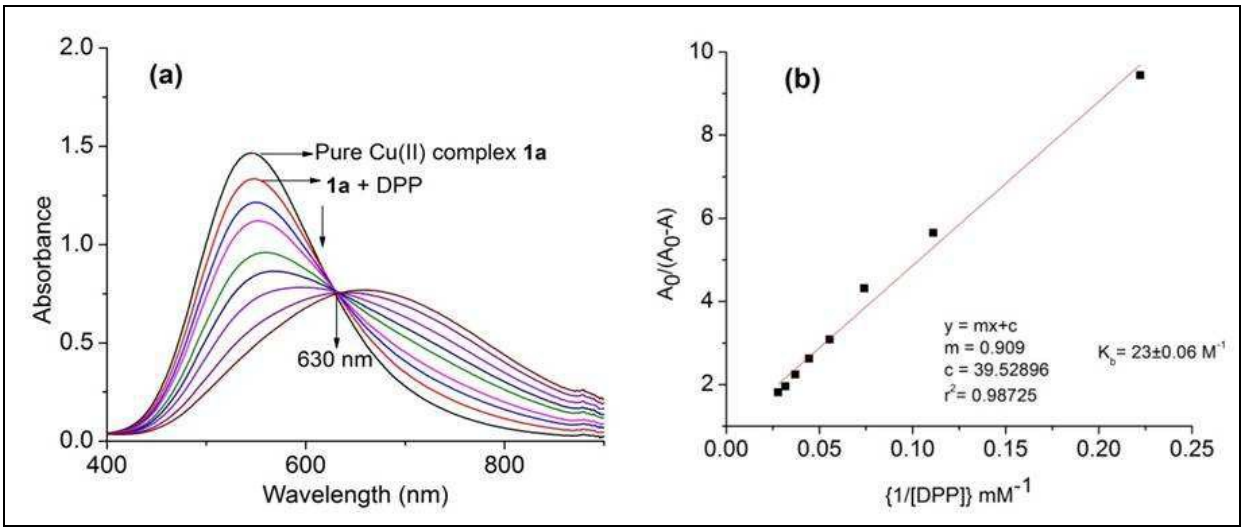

Fig. 6. (a) Electronic absorption spectral changes for the stepwise addition of DPP (25-200 µL, 0.45 M) to $[Cu(dach)_2(ClO_4)_2]$ **1a** (18 mM) in acetonitrile, (b) Linear plot for the calculation of intrinsic binding constant, K_b.

Similarly, the binding affinity of DPP to complex **2a** was studied in acetonitrile (Fig. 7a). The color of the solution changed from colorless to light yellow, with an intense absorption band at λ_{max} = 265 nm (ε = 8.7x 10^3 M^{-1} cm^{-1}). This could be due to LMCT of DPP bound Cu(II) and Zn(II) complex. The indirect support for the formation of DPP complexes can be taken from single crystal X-ray structures of analogous BNPP complexes, **3** and **4** respectively.

The binding constant K_b was calculated from the plot of $A_0/(A_0-A)$ against 1/[DPP] which yields a straight line with the ratio of the intercept to the slope equal to binding constant.[51,52] A_0 and A denote the absorbance at a particular wavelength in the absence and in the presence of DPP, respectively. The binding constants for **1a**–**1d** and **2a**–**2d** were calculated and provided in the Table 3. The results indicate that the binding strength of complex **2a** is much stronger than that of complexes **1a**–**1d** and **2b**–**2d**. The k_b values of Cu(II) complexes are comparable with the related DPP (diphenyl phosphate) (267 M^{-1}), phosphodimethylphosphate (211 M^{-1}) and HPNP (2-(hydroxypropyl)-p-nitrophenylphosphate) (190 M^{-1}) Cu(II) complexes.[34]

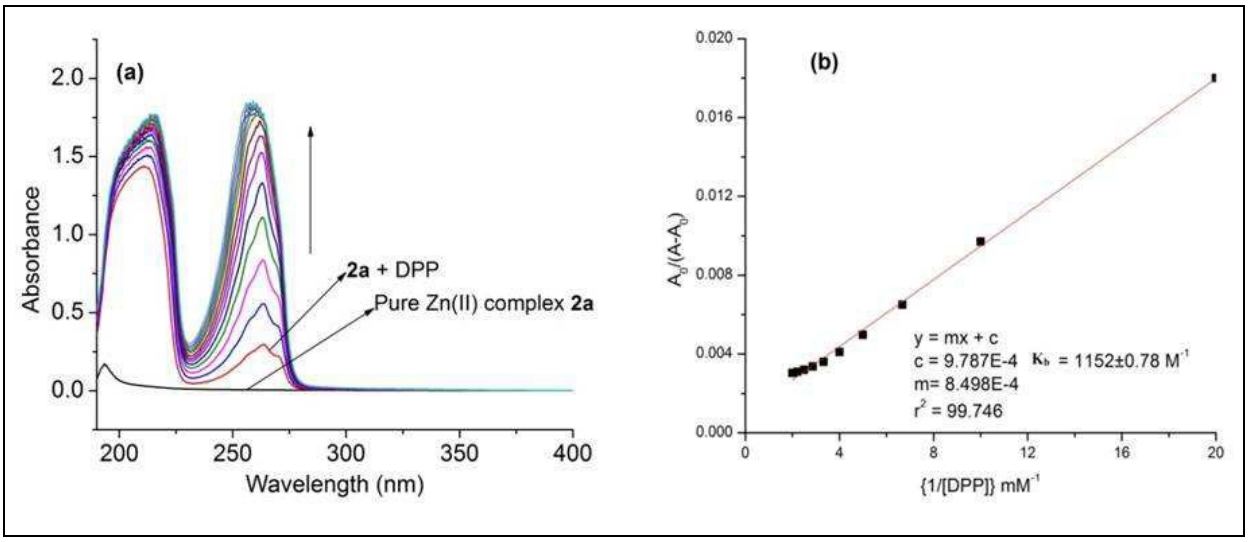

Fig. 7. (a) Electronic absorption spectral changes for the stepwise addition of DPP (10-100 µL, 0.0125 M) to $[Zn(dach)_2](ClO_4)_2$ **2a** (0.25 mM) in acetonitrile. (b) Linear plot for the calculation of intrinsic binding constant, K_b.

4.2. DNA Binding Studies by UV-Vis spectroscopy

The binding ability of the complexes **1a**–**1d** and **2a**–**2d** with CT-DNA were studied by UV-Vis spectrophotometer as it is one of the most widely used methods to investigate the interactions of metal complexes with DNA. The absorption titrations for complexes were performed with changing the concentration of DNA from 0-10 µM, by keeping the complex concentration constant (5 mM). The absorption intensity was kept on decreased upon each addition of the DNA incase of copper complexes **1a**–**1d**. The absorption was kept on increased upon each addition of the DNA incase of zinc complexes **2a**–**2d**. The absorption spectra of complexes **1b** and **2d** in the absence and presence of CT-DNA were shown in Fig. 8a and 9a. The binding constants for complexes with DNA were calculated from the following equation.[35]

$$[DNA]/|\varepsilon_a-\varepsilon_f| = [DNA]/|\varepsilon_b-\varepsilon_f|+1/K_b|\varepsilon_b-\varepsilon_f|$$

Where, [DNA] represents the concentration of the DNA, ε_a, ε_b and ε_f correspond to extinction coefficient of partially bound DNA to complex, the extinction coefficient of the free complex and the extinction coefficient of the fully bound complex to the DNA.

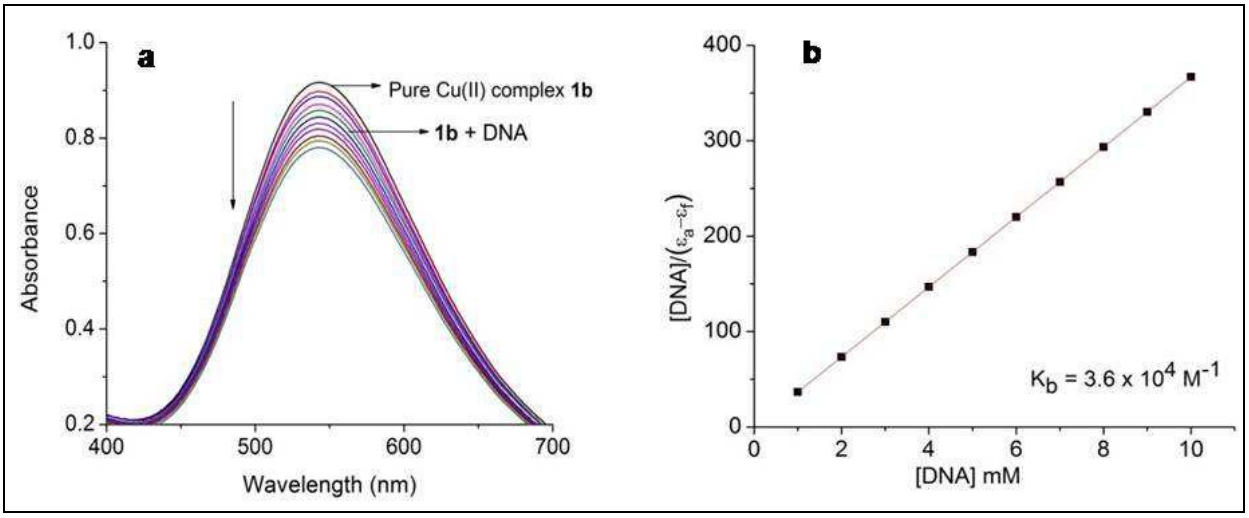

Fig. 8. (a) Absorption spectral titration of complex **1b** (5 mM) with CT-DNA (0-10 μM) (b) The plot of [DNA]/(ε_a-ε_f) Vs [DNA].

The binding constant K_b was calculated from the plot of [DNA]/ε_a-ε_f against [DNA] which yields a straight line with the ratio of the slope to the intercept equal to binding constant. The binding constants of complexes **1a**–**1d** and **2a**–**2d** were calculated, which are comparable with literature reports,[13,36] and illustrated in the Table 3.

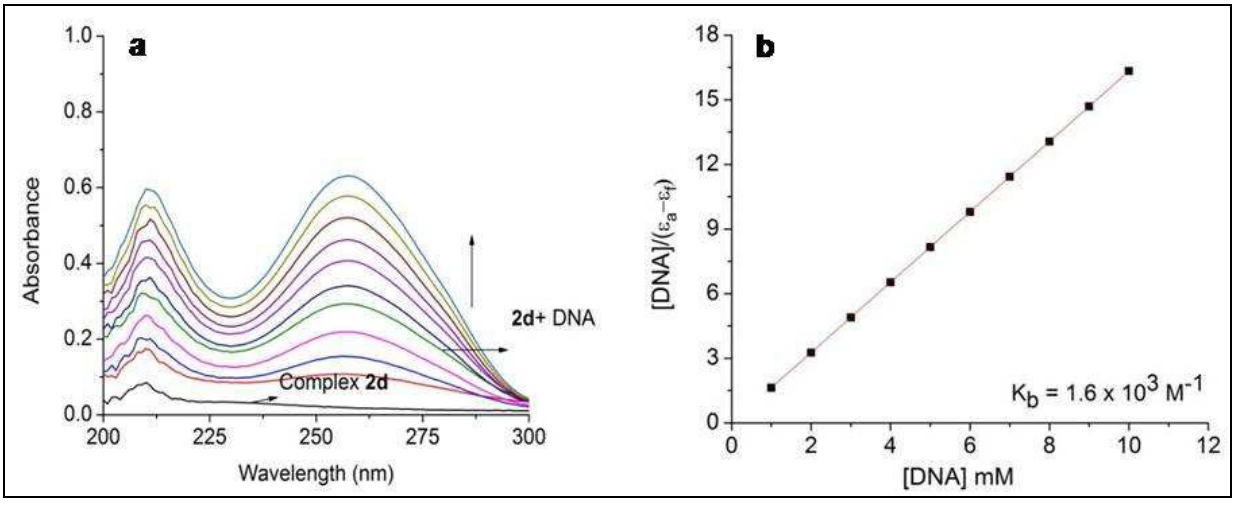

Fig. 9. (a) Absorption spectral titration of complex **2d** (5 mM) with CT-DNA (0-10 μM) (b) The plot of [DNA]/(ε_a-ε_f) Vs [DNA].

4.3. Circular Dichroism Study

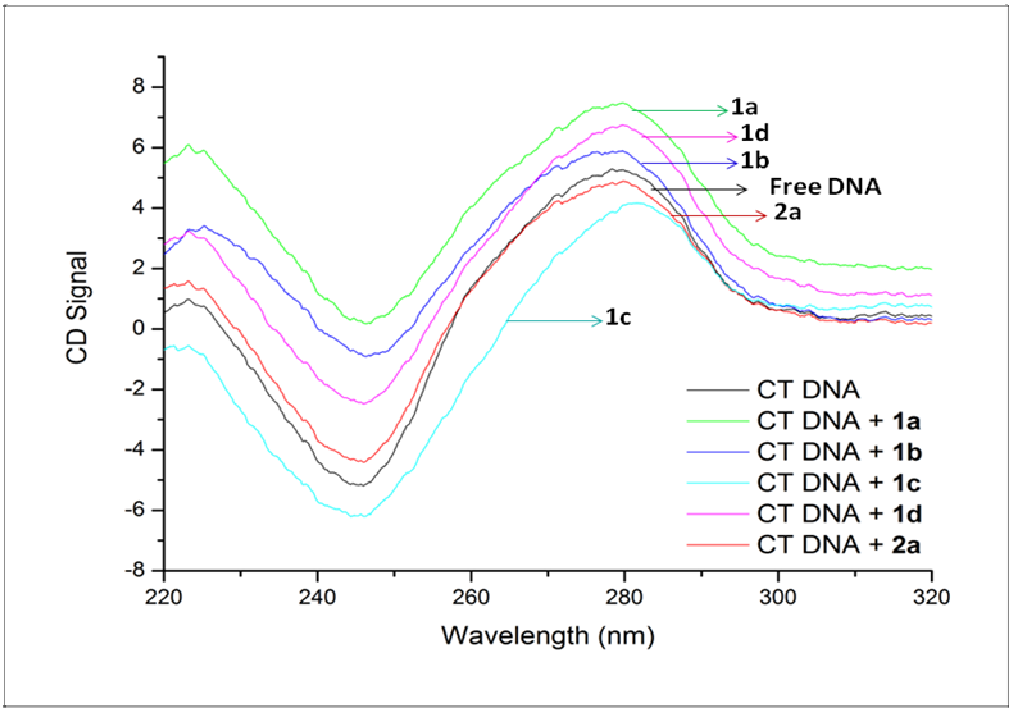

Fig. 10. CD spectra of CT DNA and its interaction with **1a-d** and **2a** where [complex]/[CT DNA] = 0.5. All spectra were recorded at room temperature in Tris/HCl buffer, pH 7.4.

The circular dichroism spectroscopy is a powerful method for investigation of the interaction between small molecules and DNA.[37,47d] It is also used for the determination of the secondary structural changes of DNA after binding with small molecules. The CD spectrum of CT-DNA demonstrates a positive band at 277 nm due to base stacking and a negative band at 245 nm due to helicity which are very sensitive to the DNA interaction with metal complexes. Small molecules interacts with DNA through groove binding/electrostatic interaction to exhibit a slight or no perturbation on the base stacking and helicity bands of DNA, while intercalation increases the intensities of both the bands as a result of right-hand B form of DNA. Complexes **1a-1d** and

2a are incubated with DNA at 1/R= [Complex]/[DNA] = 0.5 and the CD spectrum were recorded at room temperature in Tris/HCl buffer, pH 7.4. The spectra showed small changes in both positive and negative bands (Fig. 10) with slight decrease and increase in band intensities, suggesting that the interactions of complexes **1a-1d** and **2a** interrupts the CT-DNA helicity. These results are in support of minor groove binding as shown in literature reports[38,44a, 13b]

4.4. Viscosity measurements

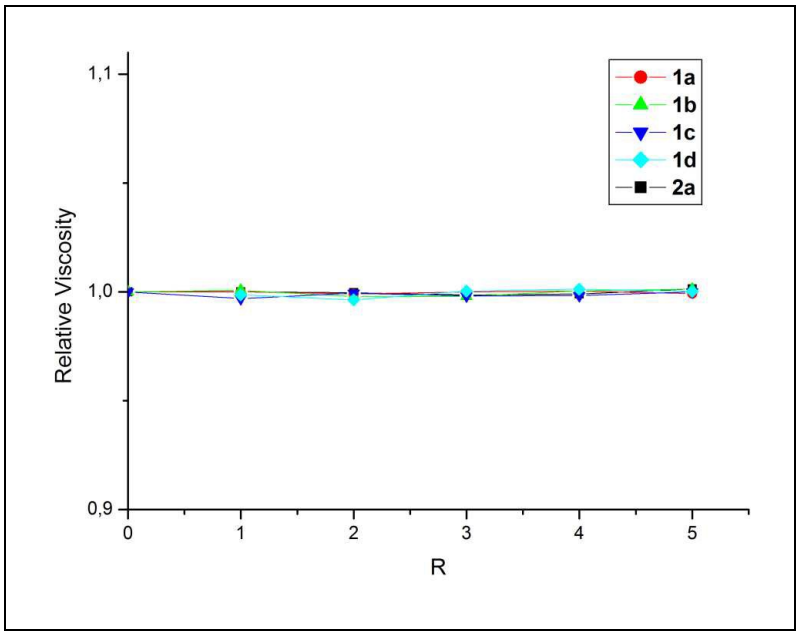

Fig. 11. Effect of the complexes **1a-d** and **2a** on the viscosity of CT DNA. Measurements were done in 10 mM Tris/HCl buffer, pH 7.4 and at 37 °C with [CT DNA] = 50 μM; *R* = [complex]/[CT DNA]; Relative viscosity (η/η_o) is plotted against *R*.

Viscosity measurement is one of the critical tests to find the mode of binding of DNA with small molecules in solution.[39,44a] When metal complexes/small molecules interact with DNA via intercalation, the viscosity of DNA increases significantly.[39a] In order to allow a suitable comparison to the aforementioned experiments, the viscosity of CT DNA solutions was measured at physiological temperature (37 °C) with varying concentrations of **1a-d** and **2a**. The relative viscosity of CT DNA doesn't show any significant changes when increasing the complex concentration, which means that the complexes do not bind with CT DNA by intercalation (Fig

11). Combined with the binding constants of **1a-1d** and **2a**, the result of the viscosity measurements implies that the complexes bind with CT DNA via groove binding or electrostatic mode.[40]

4.5. Cyclic Voltammetric studies

The redox properties of the copper complexes, **1a-1d** were investigated at pH 7.4 by cyclic voltammetry in Tris-HCl buffer with Tetrabutylammonium perchlorate as the supporting electrolyte. As a representative example, CV of complex **1a** is given in Fig. 12. It displays a quasi-reversible one-step reduction peak Epc (cathodic potential) at -0.568 V due to Cu(II)/Cu(I) and one oxidation peak Ea (anodic potential) at -0.087 V due to Cu(I)/Cu(II). The obtained redox potentials are comparable with mononuclear Cu(II) amine complexes, $[CuL(ClO_4)_2]$ and $[CuLCl_2]$ where L= *N,N′*-Bis(benzimidazole-2-ylethyl)-ethane-1,2-diamine.[41]

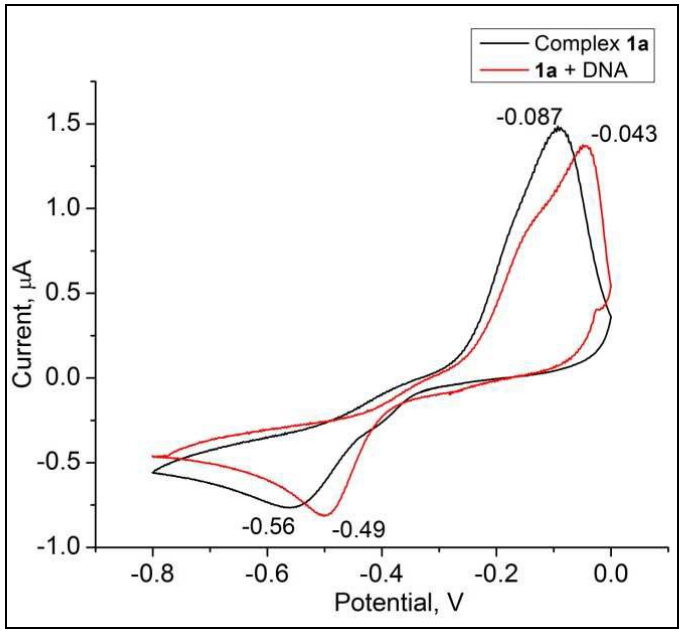

Fig. 12. Cyclic voltammogram of $[Cu(dach)_2(ClO_4)_2]$ **1a** (~1 mM) in Tris-HCl buffer at pH 7.4. $[Bu_4NClO_4]$= 10 mM; Potentials are referenced vs. Ag/AgCl; scan rate: 50 mVs^{-1}.

When redox active metal complexes interact with DNA, cyclic voltammetric technique gives valuable information regarding binding affinity.[42,25,44a,47d] The cyclic voltammograms of the complexes **1a**-**1d** in the absence and presence of CT-DNA exhibit considerable shifts in the anodic and cathodic peak potentials, indicating the binding interaction existing with DNA (Fig.12, Table 3).

The shift in the value of the formal potential (ΔE^o) was used to estimate the ratio of equilibrium binding constants K_R/K_O. Bard and Carter described the model of interaction using the following equation.[43]

$$\Delta E° = E_b° - E_f° - 0.059 \log(K_R/K_O)$$

Where $E_b°$ and $E_f°$ are the initial potentials of the bound and free complexes, respectively, and K_R and K_O are binding constants for reduction and oxidation forms to the CT-DNA. The K_{ox}/K_{red} values are 1.17, 1.04, 1.02 and 1.06 for **1a**, **1b**, **1c** and **1d,** respectively. The results suggest that all Cu(II) complexes exhibit similar binding affinity with CT-DNA via groove binding/electrostatic interaction.[40a]

Table 3: Cyclic Voltammetric Data of the complexes **1a**-**1d**.

Complex	Redox couple	Ipc (A) × 10^{-5}		Epc (V)		$E_{1/2}$ (V)		ΔEp (V)		K_{ox}/K_{red}
		Free	Bound	Free	Bound	Free	Bound	Free	Bound	
1a	Cu(II)/Cu(I)	4.3	6.1	-0.56	-0.49	-0.323	-0.266	0.473	0.447	1.17
1b	Cu(II)/Cu(I)	0.72	1.4	-0.603	-0.586	-0.318	-0.356	0.568	0.459	1.04
1c	Cu(II)/Cu(I)	0.6	0.73	-0.584	-0.574	-0.335	-0.32	0.496	0.505	1.02
1d	Cu(II)/Cu(I)	0.8	1.5	-0.591	-0.564	-0.332	-0.326	0.517	0.476	1.06

4.6. DNA cleavage studies

DNA cleavage studies were carried out in the absence and presence of ascorbate as a reducing agent. For the Cu(II) containing compound **1a** redox chemistry is expected to be involved in the cleavage process. In the case of the Zn(II) complex **2a**, ascorbate was also added in some samples for the sake of comparison. To assess the DNA cleavage ability of the

complexes supercoiled (sc) pBR322 DNA (Form I) was incubated with varying concentrations of **1a** and **2a** in Tris-HCl buffer (50 mM) at pH 7.4 for 2 h in the presence and absence of ascorbate.

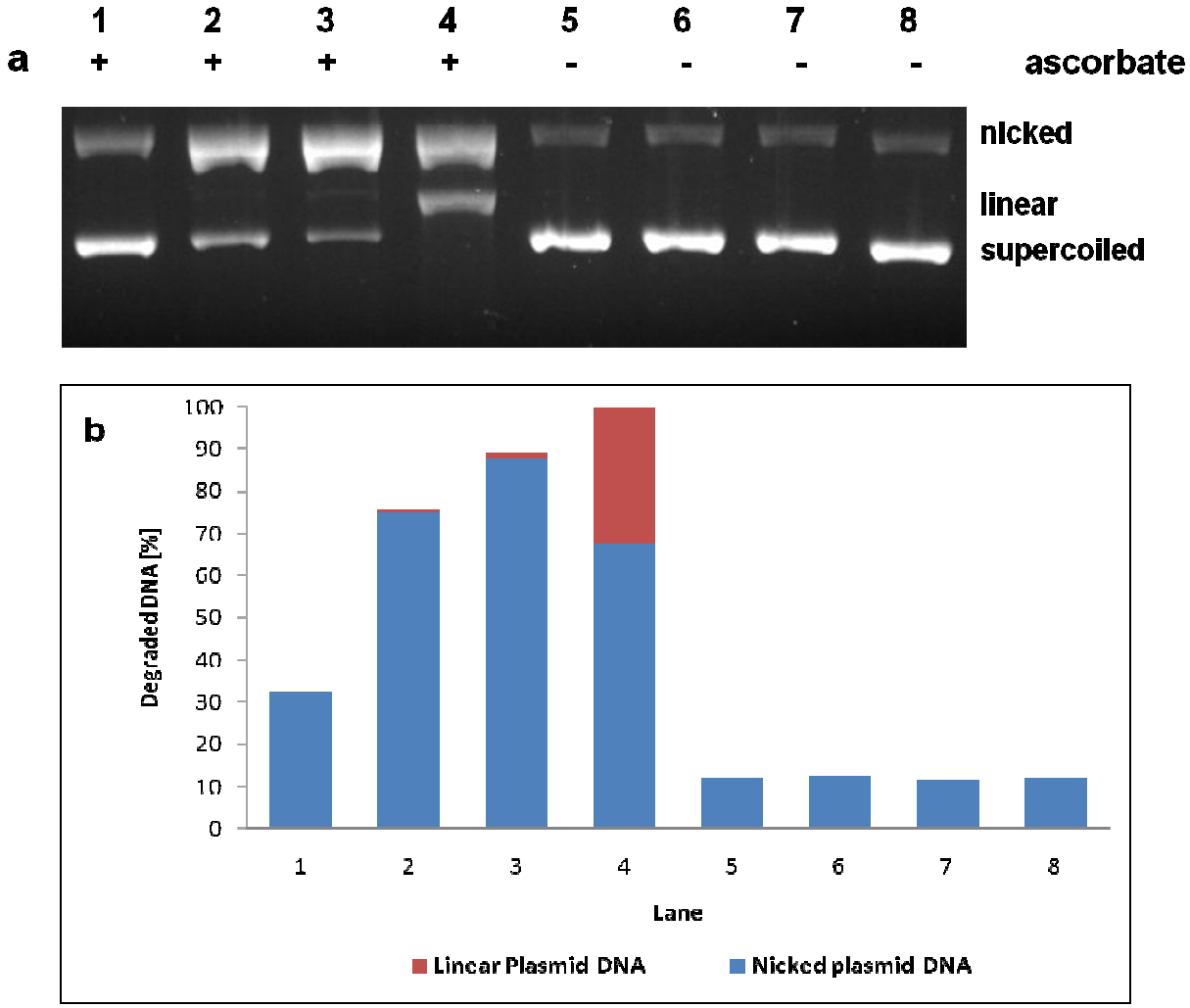

Fig. 13. (a) Cleavage activity of **1a** monitored by 1% agarose gel electrophoresis. Every lane contained 0.2 μg plasmid DNA in 50 mM Tris-HCl buffer (pH 7.4). Lane 1: 1 mM ascorbate and reference DNA; lane 2-4: 1 mM ascorbate+ **1a** (6.3, 12.5 & 25 μM, respectively); lane 5-7: **1a** (6.3, 12.5 & 25 μM, respectively); lane 8: reference DNA. (b) Percentage of degraded DNA.

At 3.1–12.5 μM concentration and in the presence of ascorbate, **2a** caused DNA damage (Fig. 14, lanes 2-4) in the same range as the ascorbate containing control (lane 1), thus indicating that the Zn(II) complex **2a** does not cleave DNA under the conditions applied. In the absence of

ascorbate, **2a** does not cause any significant DNA cleavage either (Fig. 14). Although phosphate binding was observed (see X-ray structure and UV/Vis results above), the complex is not able to cleave DNA.

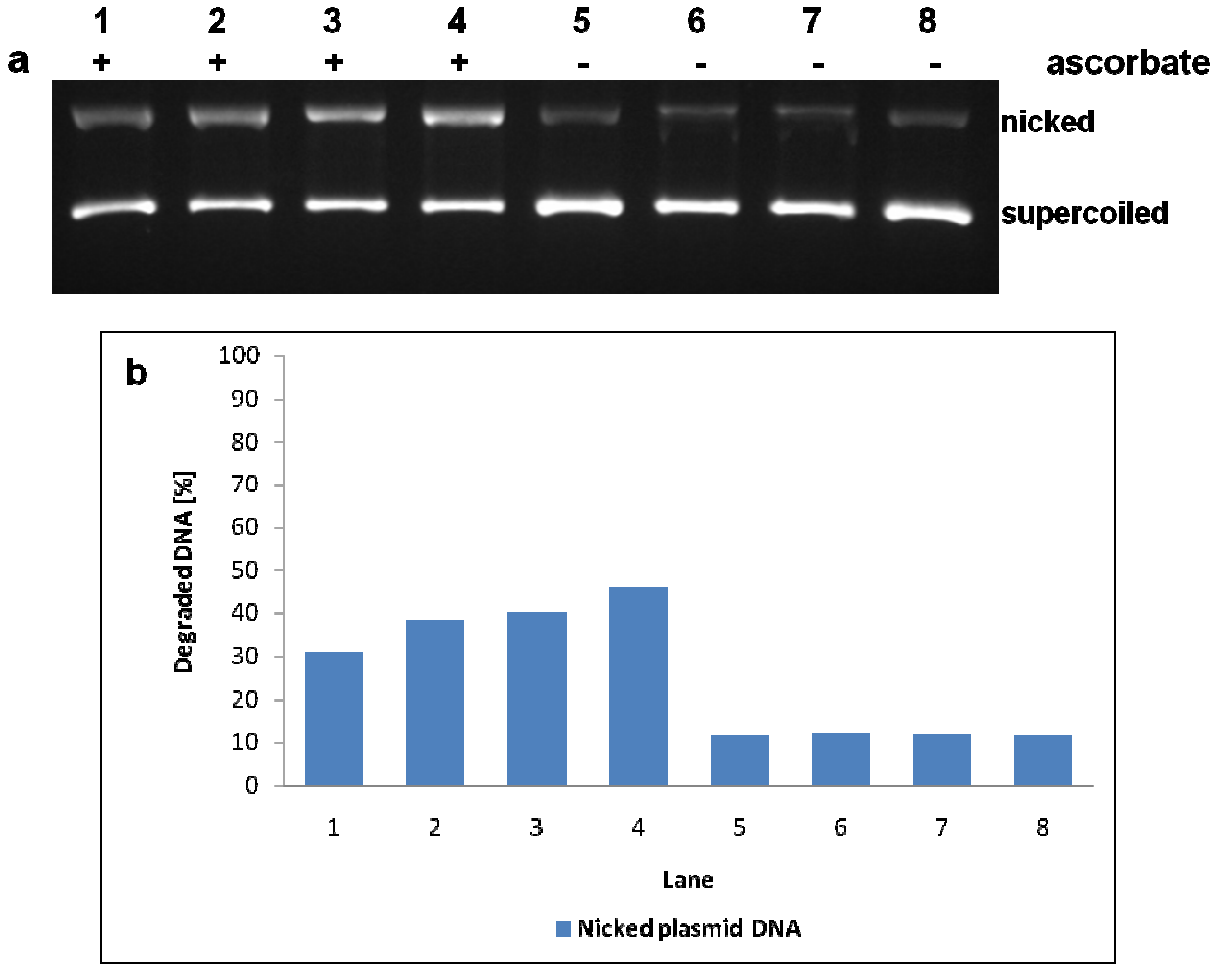

Fig. 14. (a) Cleavage activity of **2a** monitored by 1% agarose gel electrophoresis. Every lane contained 0.2 µg plasmid DNA in 50 mM Tris-HCl buffer (pH 7.4). Lane 1: 1 mM ascorbate and reference DNA; lane 2-4: 1 mM ascorbate+ **2a** (3.1, 6.3 & 12.5 µM, respectively); lane 5-7: **2a** (3.1, 6.3 & 12.5 µM, respectively); lane 8: reference DNA. (b) Percentage of degraded DNA.

In contrast to complex **2a**, cleavage activity of **1a** in the presence of ascorbate was observed (Fig. 13). At 6.3 µM and 12.5 µM concentration, cleavage by complex **1a** yields 1% and 3% of linear plasmid DNA (Form III), whereas at a higher concentration of 25 µM, **1a**

produced complete cleavage of the supercoiled DNA into 67% of Form II (open circular/nicked) and 33% of Form III (linear). Above 25 μM of **1a**, the supercoiled DNA was cleaved into small fragments, which led to the disappearance of the bands (not shown). In the absence of ascorbate, **1a** did not cause any significant DNA cleavage (lanes 5-7).

It has to be taken into account that complex **1a** contains dach as a diasteromeric mixture of *trans- and cis*-dach. In order to investigate if the stereochemistry of the dach ligand had any influence on the cleavage activity of the chiral DNA molecule, (*R*,*R*)-*trans*-(**1b**), (*S*,*S*)-*trans*-(**1c**) and *cis*-dach (**1d**) Cu(II) complexes were applied for DNA cleavage. As expected they do not show significant cleavage in the absence of ascorbate, whereas at low concentrations in the presence of ascorbate, these complexes show only slightly higher activity. In the presence of ascorbate and at 25 μM, complex **1b** produces complete cleavage of the supercoiled DNA into 20% of Form II and 80% of Form III. **1c** produces 42% of Form II and 58% of Form III, whereas the cleavage by **1d** yields 49% of Form II and 51% of Form III. All results are summarized in Table 4.

Table 4

Binding and DNA cleavage studies of the complexes **1a-1d** and **2a-2d**

S. No	Complex[a]	DPP (k_b M^{-1})	DNA (k_b M^{-1})	DNA cleavage		
				Conc. μM	Form II	Form III
1	[Cu(*cis/trans*-dach)$_2$(ClO$_4$)$_2$]**1a**	23	4.5×10^3	25	67%	33%
2	[Cu((*R*,*R*)-*trans*-dach)$_2$(ClO$_4$)$_2$] **1b**	28	3.6×10^4	25	20%	80%
3	[Cu((*S*,*S*)-*trans*-dach)$_2$(ClO$_4$)$_2$] **1c**	29.6	4.2×10^4	25	42%	58%
4	[Cu(*cis*-dach)$_2$(ClO$_4$)$_2$] **1d**	61.7	1.6×10^4	25	49%	51%
5	[Zn(*cis/trans*-dach)$_2$(ClO$_4$)$_2$] **2a**	1150	0.9×10^3	-	-	-
6	[Zn((*R*,*R*)-*trans*-dach)$_2$(ClO$_4$)$_2$] **2b**	186	2.7×10^4	-	-	-
7	[Zn((*S*,*S*)-*trans*-dach)$_2$(ClO$_4$)$_2$] **2c**	376	2.4×10^4	-	-	-
8	[Zn(*cis*-dach)$_2$(ClO$_4$)$_2$] **2d**	339	1.6×10^3	-	-	-

[a]*cis/trans*-dach=*cis/trans*-1,2-diaminocyclohexane,(*R*,*R*)-*trans*-dach=(*R*,*R*)-*trans*-1,2-diaminocyclo-hexane, (*S*,*S*)-*trans*-dach= (*S*,*S*)-*trans*-1,2-diaminocyclohexane, *cis*-dach= *cis*-1,2-diaminocyclohexane.

In comparison to established Cu(II) based DNA cleaving agents, however, **1b** represents a very efficient DNA cleaver. A dach tryptophan Cu(II) complex reported before required a ten-fold concentration of metal complex to achieve comparable results in the presence of ascorbate.[17,44,45] Recently N. Kulak, et.al reported that Cu(II) complexes of hetero substituted cyclen ligand at 80 μM shows CT DNA cleavage up to 90% to that of only Form II.[16b] The significant increase of activity for **1b**, (*R,R*)-*trans*-dach Cu(II) complex) might be due to convenient interactions of this enantiomer with plasmid DNA indicating enantio selectivity for the cleavage process. In the absence of ligand, DNA cleavage activity of simple copper(II) salt, $Cu(ClO_4)_2.6H_2O$ shows only 15% of form III under identical conditions.

4.7. Quenching studies.

In order to characterize the reactive oxygen species responsible for the DNA cleavage of **1a**, different scavengers were used; *tert*-butanol and DMSO for hydroxyl radicals, sodium azide (NaN_3) for singlet oxygen, catalase for hydrogen peroxide, superoxide dismutase for superoxide (Fig. 15).

The strongest quenching effect for the DNA cleavage when compared to the undisturbed sample (lane 2) was observed in the presence of catalase (lane 6). From this it can be concluded that hydrogen peroxide might be the reactive species responsible for DNA cleavage.[28b,46,47] DMSO shows a weak quenching effect, whereas a very weak quenching effect was apparent in the presence of *tert*-butanol and sodium azide. As a result, the involvement of hydroxyl radicals and singlet oxygen as reactive species cannot be excluded. According to Sigman et al. H_2O_2 can be generated by reaction of Cu(I) with O_2. Cu(I) itself is generated by reacting with a reducing agent, here ascorbate.[48]

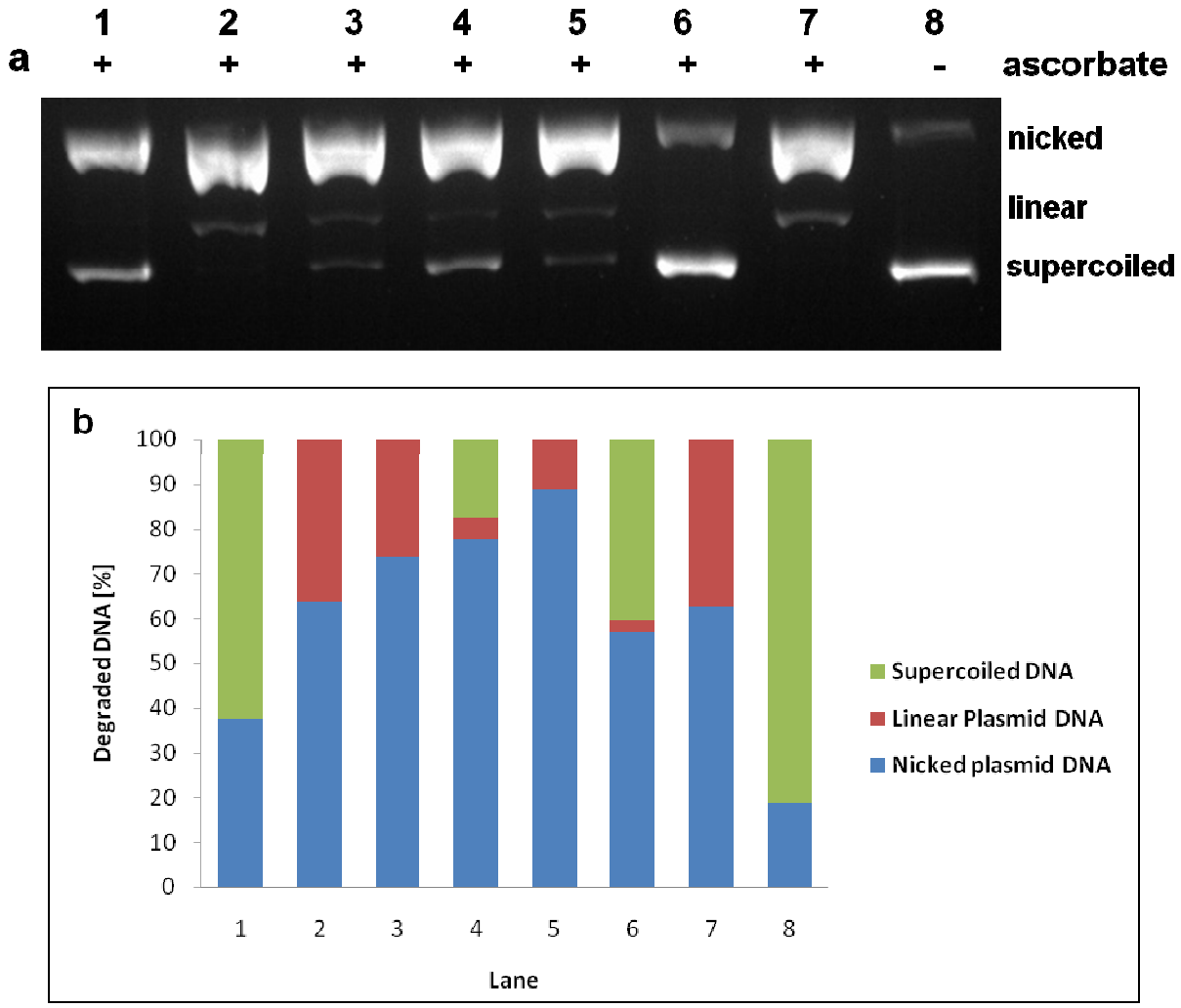

Fig. 15. (a) Quenching effects of DNA cleavage by **1a** monitored by 1% agarose gel electrophoresis. Every lane contained 0.2 µg plasmid DNA. Lane 1-7 contained 1 mM ascorbate and 0.25x PBS in 50 mM Tris-HCl buffer (pH 7.4). Lane 2-7 contained 25 µM of **1a**. Lane 1: reference DNA (negative control); lane 2: reference (positive control); lane 3: 200 mM *tert*-BuOH; lane 4: 200 mM DMSO, lane 5: 10 mM NaN_3; lane 6: 2.5 mg/mL catalase; lane 7: 5 units of superoxide dismutase; lane 8: reference DNA. (b) Percentage of degraded DNA.

Similarly, the activity of complexes **1b**–**1d** was quenched by hydrogen-peroxide scavenging catalase. All other scavengers did not cause significant quenching effects of the DNA cleavage (except for *tert*-BuOH in the case of **1c**, for which there is no plausible explanation).

5. Conclusions

In conclusion, we have synthesized mononuclear complexes $[Cu(dach)_2(ClO_4)_2]$ **1a** and $[Zn(dach)_2](ClO_4)_2$ **2a** with simple 1,2-diaminocyclohexane (*cis/trans*-dach) ligands incliding stereo isomeric compounds with (*R,R*)-*trans* (**1b**, **2b**), (*S,S*)-*trans* (**1c**, **2c**) and *cis*-dach (**1d**, **2d**). The complexes were thoroughly characterized by routine spectroscopic and single crystal XRD techniques. The intrinsic binding constant values indicate that **2a** binds more avidly to phosphodiesters such as BNPP and DPP than **1a**-**1d** and **2b**-**2d**. CD spectral studies implies that all complexes involved in groove binding with CT-DNA. Viscosity measurements suggest that increasing complex concentration does not show any significant influence on the viscosity of DNA. Cyclic voltammetric analyses reveal similar binding affinity of **1a-d** with CT-DNA. All these studies support for groove binding/electrostatic interaction with CT-DNA. The oxidative DNA cleavage by complexes **1a**-**1d** and **2a**-**2d** with pBR322 DNA was evaluated by agarose gel electrophoresis; noticeably, the complex **1b** exhibits effective DNA cleavage at 25 uM very efficiently up to 80% linear form. Our results suggest that complex **1b** is effective DNA cleaver compared to many mononuclear Cu(II) complexes with N-donor ligands which act as DNA cleaving agents at higher concentration.[17c, 36b,c] The present study also supports for efficient binding affinity of zinc complexes **2a**-**2d** towards phosphodiesters.

6. Experimental Section

6.1. Materials

Cu(II) and Zn(II) salts and other chemicals were commercially available (Aldrich and Fluka) in high purity. Plasmid DNA pBR322 was purchased from *Carl Roth GmbH*. CT-DNA was purchased from Aldrich. All reagent grade compounds were used without further purification. Solvents were dried and distilled by standard procedures.[49]

6.2 Physical measurements

C, H, N analysis was performed on a Thermo Scientific FLASH 2000 Organic Elemental Analyzer. Electronic absorption spectra were recorded on an UV-2450 Model instrument and FT-IR spectra with KBr disks on a Shimadzu IR-470 spectrophotometer. NMR spectra were recorded on a Bruker Avance-400 spectrometer. EPR spectra were obtained from a Varian E-112 X-band spectrophotometer. The CD spectra were measured with J-815 Cercular Dicroism Spectrophotometer. The Viscosity measurements were carriedout with Ubbelohde Viscometer. Electrochemical measurements were performed on Autolab type (PGSTAT 302N) electrochemical analyzer. A cell equipped with a glassy carbon working electrode, a Pt-wire auxiliary electrode and Ag/AgCl reference electrode. The complex solution was deoxygenated by bubbling of high purity nitrogen. For the characterization of the synthesized compounds, mass spectral data were measured with the device Agilent 6210 (ESI-TOF, 4 kV), from Agilent Technologies.

6.3. DNA Binding Studies

Binding experiments were carried out by using UV-Vis spectrophotometer. All the compounds were dissolved in the 10 mM Tri-HCl buffer (7.4 pH) and the concentration of the DNA was determined from the UV absorption intensity at 260 nm with $\varepsilon = 6600\ M^{-1}cm^{-1}$.[50] The DNA solution in Tris-HCl buffer gave a ratio at 260 and 280 nm of about 1.8-1.9 which is indicating that the CT-DNA was sufficiently free of protein. In this study, the DNA concentration was increasing from 0-10 μM and complex concentration was kept constant.

6.4. Circular Dichroism Studies

The CD spectra were measured with a continuous flow of nitrogen purging the polarimeter at room temperature with 1 cm pathway cells. The CD spectra were run from 320 to 220 nm at 100 nm/min and the buffer background was subtracted automatically. Data were recorded at 0.1 nm intervals. The CD spectrum of CT-DNA (100 μM) alone was recorded as the control experiment. 50 μM of complexes (**1a-1d** and **2a-2d**) concentration was used used for recording the CD spectra.

6.5. Viscosity measurements

The viscosity of CT DNA solutions was measured at 37 ± 0.1 °C using an Ubbelohde viscometer. In order to detect the viscosity of the solution, 15 mL of 10 mM Tris/HCl buffered solution and of 50 μM CT DNA was taken to the viscometer and a flow time reading was obtained. An appropriate amount of one of the complexes **1a-1d** or **2a** was added to the viscometer to give a certain ratio value while keeping the CT DNA concentration constant, and the flow time was read. The flow times of samples were measured after the achievement of thermal equilibrium (30 min). Each point measured was the average of five readings. The obtained data were presented as relative viscosity η/η_o versus *R*, where η is the reduced specific viscosity of DNA in the presence of a complex and η_o is the reduced specific viscosity of CT DNA alone.

6.6. Cyclic voltammetry

Electro chemical measurements were performed in a single compartmental cell. A cell equipped with a glassy carbon working electrode, a Pt-wire auxiliary electrode and Ag/AgCl reference electrode. The complex solution was deoxygenated by bubbling of high purity nitrogen. All the measurements were carried out in Tris-HCl buffer with Tetrabutyl ammonium

perchlorate as a supporting electrolyte at 25 °C. The Nernst equation was used to calculate the ratio of equilibrium constants for the binding of Cu(I) and Cu(II) ions to DNA.[43]

$$E_b° - E_f° - 0.059 \log(K_R/K_O)$$

Where $E_b°$ and $E_f°$ are the initial potentials of the bound and free complexes, respectively, and K_R and K_O are binding constants for reduction and oxidation forms to the CT-DNA.

6.7. DNA cleavage experiments

The DNA cleavage experiments of the complexes **1a-1d** and **2a-2d** were performed with 0.2 μg DNA. Incubation of the samples were performed in 50 mM Tris-HCl buffer (pH 7.4) at 37 °C for 2 h. After incubation, DNA samples were run on horizontal agarose gels (1%) containing ethidium bromide (2 μg/mL) in 0.5x TBE buffer for 2 h at 40 V. Quantization of closed circular, nicked, and linear DNA was made via analysis of ethidium bromide containing agarose gels by fluorescence imaging on a *Bio-Rad* Gel Doc EZ Imager. Data analysis was performed with Image Lab 3.0 software. DNA was incubated at the same conditions as described above in the presence of either 200 mM *tert*-butanol, 200 mM DMSO, 10 mM NaN_3, 2.5 mg/mL catalase (from bovine liver, 2-5 units/μL) or 5 units/μL of superoxide dismutase. Addition of 2X phosphate buffered saline (PBS) to all samples (except for the reference) was necessary because catalase had to be pre-incubated at 37 °C in 1X PBS for 30 min. The resulting PBS concentration in every incubation mixture amounts 0.25X altogether.

Cleavage experiments were conducted three times. In the bar diagrams the average of three experiments is given, whereas the respective gel shown is one representative gel out of three.

6.8. Electronic absorption titration with DNA models

Absorption spectra were recorded on a UV-Vis spectrophotometer using 1 cm quartz cuvettes. Absorption titrations were performed by keeping the concentration of the complex

constant and by varying the concentration of DPP. While measuring the spectra, an equal amount of DPP was added to the metal complex. The binding constant (K_b) for the binding of the complex with DPP, was determined from the spectroscopic titration data using the Benesi-Hildebrand equation, through plot of $A_0/(A_0-A)$ against 1/[DPP] which yields a straight line with the ratio of the intercept to the slope gave the value of the binding constant,[45,46] where A_0 and A denote the absorbance at a particular wavelength in the absence and in the presence of DPP, respectively.

6.9. X-Ray crystallography

X-Ray crystallographic studies were carried out on an X calibur Oxford Diffraction Ltd. with Mo-Kα radiation (λ = 0.71073 Å). Structure solution and refinement were performed with SHELX-97.[53] All non-hydrogen atoms were refined anisotropically. Hydrogen atoms were generated according to stereochemistry and refined using riding model in SHELX-97. X-ray crystal data were collected on Crystallographic data collection and refinement parameters are shown in Table 2.

6.10. Synthesis of metal complexes

Safety Note: Caution! Metal complexes of perchlorate salts are potentially explosive and should be handled with care.

6.10.1. Synthesis of $[Cu(dach)_2(ClO_4)_2]$ (1a)

To a solution of copper perchlorate hexahydrate (0.97 g, 2.62 mmol) in methanol (3 mL) was added the solution of the ligand dach (*cis*/*trans* mixture) (0.6 g, 5.25 mmol) in the same solvent (3 mL). A purple color precipitate that formed was stirred for 2 h, filtered and dried in *vacuo* to yield **1a** (1.37 g, 87%). X-ray quality crystals were obtained by slow evaporation of solution of the complex **1a**, in acetonitrile. The unit cell parameters of this crystal matches with

that of reported one (19 a). Anal.Calcd. for $C_{12}H_{28}Cl_2CuN_4O_8$ (490.82): C, 29.35; H, 5.75; N, 11.42. Found: C, 29.42; H, 5.70; N, 11.37%. UV-Vis (CH_3CN); λ_{max}, 546 nm (ε = 92 M^{-1} cm^{-1}). FT-IR (KBr, cm^{-1}): 3323, 3267, (ν_{N-H}, stretching); 2932, (ν_{C-H}, stretching); 1080 (bs), $\nu(ClO_4)$. ESI-MS: $[Cu(dach)_2ClO_4]^+$ m/z = 390.1207, calcd = 390.1095; $[Cu(dach)ClO_4]^+$ m/z = 275.9960, calcd = 275.9938.

6.10.2. Synthesis of copper complexes (1b-1d)

Complexes **1b-1d** were synthesized by following the above procedure by using copper perchlorate hexahydrate and appropriate enatio-pure-1,2-diaminocyclohexane to obtain **1b** (81%), **1c** (77%) and **1d** (93%) yields. UV, IR, Elemental analysis and ESI-MS values of all complexes are matching with complex **1a**.

6.10.3. Synthesis of $[Zn(dach)_2](ClO_4)_2$ (2a)

To a solution of zinc perchlorate hexahydrate (0.3 g, 0.8 mmol) in methanol (3 mL), was added the solution of the ligand dach (*cis*/*trans* mixture) (0.184 g, 1.6 mmol) in the same solvent (3 mL). A white precipitate that formed was stirred for 2 h, filtered and dried in *vacuo* to yield **2a** (0.433 g, 88%). X-ray quality crystals were obtained by slow evaporation of solution of the complex **2a**, in methanol. Anal.Calcd. for $C_{12}H_{28}Cl_2ZnN_4O_8$ (492.66): C, 29.95; H, 5.32; N, 11.47. Found: C, 29.90; H, 5.42; N, 11.52%. ^{1}H NMR (δ, DMSO-d_6, 400 MHz, 298 K): 2.09 (m, 2H), 1.19 (m, 4H), 1.92(m, 4H, NH_2), 1.66 (m, 4H); ^{13}C NMR (δ, DMSO-d_6, 400 MHz): 24, 28, 60 (C-NH_2) ppm. UV-Vis (CH_3CN; λ_{max}, 276 nm (ε =16.4, M^{-1} cm^{-1}). FT-IR (KBr, cm^{-1}): 3363 (ν_{N-H}, stretching); 1010 (bs), $\nu(ClO_4$, symmetric stretching); 1150 (s), $\nu(ClO_4$, Asymmetric stretching); 635 (s), $\nu(ClO_4$, Asymmetric bending); 460 (s), $\nu(ClO_4$, Asymmetric bending). ESI-MS: $[Zn(dach)_2ClO_4]^+$*m/z* = 391.1137, calcd = 391.1091; $[Zn(dach)ClO_4]^+$*m/z* = 276.9960, calcd = 276.9934.

6.10.4. Synthesis of Zinc complexes (2b-2d)

Complexes **2b-2d** were synthesized by following the above procedure by using zinc perchlorate hexahydrate and appropriate enatio-pure-1,2-diaminocyclohexane to obtain **2b** (83%), **2c** (80%) and **2d** (91%) yields. UV, IR, Elemental analysis and ESI-MS values of all complexes are matching with complex **2a**.

6.10.5. Synthesis of $[Cu(dach)_2(BNPP)_2]$ (3)

To a solution of copper complex **1a** (0.05 g, 1.02 mmol) in acetonitrile (3 mL) was added the solution of the ligand BNPP (0.073 g, 2.04 mmol) in the same solvent (3 mL). A white precipitate that formed was stirred for 7 h at 50 ^{0}C, filtered and dried in *vacuo* to yield **3** (0.072 g, 63%). X-ray quality crystals were obtained by slow evaporation of solution of the complex **3**, in acetonitrile:water (1:1 ratio). Anal.Calcd. for $C_{36}H_{44}CuP_2N_8O_{16}$ (970.28): C, 44.56; H, 4.57; N, 11.55. Found: C, 44.60; H, 4.52; N, 11.54%. UV-Vis (CH_3CN; λ_{max}, 548 nm (ε = 58.2, M^{-1} cm^{-1}). FT-IR (KBr, cm^{-1}): 3363 (ν_{N-H}, stretching); 1257 ($\nu_{P=O}$, stretching); 907 (ν_{P-O}, stretching); 1107-1222 (ν_{C-O}, stretching).

6.10.6. Synthesis of $[Zn(dach)_2(BNPP)_2]$ (4)

To a solution of zinc complex **2a** (0.1 g, 0.2 mmol) in H_3CCN/H_2O (1:1 v/v), was added the solution of BNPP (0.197 g, 0.4 mmol) in the same solvent. A white precipitate that formed was stirred for 7 h at 50 ^{0}C, filtered and dried in *vacuo* to yield **4** (0.1 g, 51%). X-ray quality crystals were obtained by slow evaporation of solution of the complex **4**, in H_3CCN/H_2O (1:1 v/v). Anal.Calcd. for $C_{36}H_{44}ZnP_2N_8O_{16}$ (972.12): C, 44.48; H, 4.56; N, 11.52. Found: C, 44.51; H, 4.59; N, 11.55%. ^{1}H NMR (δ, DMSO-d_6, 400 MHz, 298 K): 8.1-7.4 (m, aromatic C-H), 2.09 (m, 2H), 1.19 (m, 4H), 1.66(m, 4H, NH_2); ^{13}C NMR (δ, DMSO-d_6, 400 MHz): 24, 30, 62 (C-NH_2) ppm. UV-Vis (CH_3CN; λ_{max}, 285 nm (ε = 40.6×10^3 M^{-1} cm^{-1}). FT-IR (KBr, cm^{-1}): 3363

(ν_{N-H}, stretching); 1511 (ν_{N-H}, bending); 3246 ($\nu_{C=C-H}$, stretching); 1591 ($\nu_{C=C}$, stretching); 1283 (ν_{NO2}). 1265 ($\nu_{P=O}$, stretching); 910 (ν_{P-O}, stretching); 1109-1219 (ν_{C-O}, stretching).

Acknowledgments

We are grateful to Pondicherry University for support of this project from start-up grant. Popuri Sureshbabu thanks the CSIR New Delhi for Junior Research Fellowship (JRF). We thank the Central Instrumentation Facility, Pondicherry University, for NMR spectra and DST-FIST for single-crystal X-ray diffraction facility. We thank Mr. Ganesh for single crystal X-ray data collection.

References

1. (a) R. Wang, Y. Song, J. Zan, H. Yan and Z. L. Lu, *Org. Biomol. Chem*., 2012, **10**, 7714–7720; (b) H. Shun, N. Satoshi, P. Anangamohan and M. Takashi, *Inorg. Chem*., 2011, **50**, 11437–11445.
2. (a) P. R. Reddy and A. Shilpa, *Polyhedron*, 2011, **30**, 565–572; (b) R. Ott and R. Kramer, *Eru. J. Appl. Microbiol*. *Biotechnol*., 1999, **52**, 761–767; (c) B. Iris, K. Larisa, R. R. Kramer, O. Thomas and M. Andriy, *Bioorg*. *Med. Chem. Lett*., 2006, **16**, 2781–2785.
3. (a) I. Boll, E. Jentzsch, R. Kramer and A. Mokhir, *Chem. Commun*., 2006, 3447–3449; (b) M-D. Tsai and T-T. Chang, *J. Am. Chem. Soc*., 1980, **102**, 5418–5419; (c) S. J. Lippard, *Nat.Chem. Biol*., 2006, **2**, 504–507.
4. (a) S. K. Silverman, *Angew. Chem. Int. Ed*., 2010, **49**, 7180–7201; (b) R. Ren, P. Yang, W. Zheng and Z. Hua, *Inorg. Chem*., 2000, **39**, 5454–5463.
5. (a) T. Linda, J. Tanmaya, J. Brugger and B. Graham, S. *Leone*, *Inorg. Chem*., 2011, **50**, *62*1–635; (b) F. M. Mark and R. S. Brown, *J. Org. Chem*., 2010, **75**, 8471–8477.
6. (a) S. Sabiah, B. Varghese and N. N. Murthy, *Chem. Commun*., 2009, 5636–5638; (b) H.

Qiuxia, Z. Lejie, H. Cheng, N. Jiangyang and D. Chunying, *Inorg. Chem*., 2012, **51**, 5118–5127.

7. (a) F. H. Westheimer, Science, 1987, **235**, 1173–1178; (b) N. H. Williams, B. Takasaki and M. Wall, *J. Chin, Acc. Chem. Res*., 1999, **32**, 485–493; (c) D. S. Sigman, A. Mazumder and D. M. Perrin, *Chem. Rev*., 1993, **93**, 2295–2316; (c) X. Sheng, X M. Lu, Y. T. Chen, G. Y. Lu, J. J. Zhang, Y. Shao, F. Liu and Q. Xu, *Chem. Eur. J*., 2007, **13**, 9703–9712.
8. C. H. B. Chen, L. Milne, R. Landgraf, D. M. Perrin and D. S. Sigman, *Chem Bio Chem*., 2001, **2**, 735–740.
9. F. Mancin, P. Scrimin, P. Tecilla and U. Tonellato, *Chem. Commun*., 2005, 2540–2548.
10. (a) F. Mancin and P. Tecilla, *New J. Chem*., 2007, **31**, 800–817; (b) C. Wende, C. Ludtke and N. Kulak, *Eur. J. Inorg. Chem*., 2014, 2597–2612.
11. P. Rabindra Reddy ans N. Raju, *Polyhedron*, 2012, **44**, 1–10.
12. P. Uma Maheswari, M. Van der Ster, S. Simon, B. Sharief, P. V. W. Gilles, M. Chiara, R. Sudeshna, H. Dulk, G. Patrick and J. Reedijk, *Inorg. Chem*., 2008, **47**, 3719–3727.
13. (a) L. Rangasamy, S. Ramakrishnan, E. Suresh, A. Riyasdeen, M. Abdulkadhar Akbarsha and M. Palaniandavar, *Inorg. Chem*., 2012, **51**, 5512–5532; (b**)** J. He, J. Sun, Z. W. Mao, L.N. Ji and H. Sun, *J. Inorg. Biochem*., 2009, 103, 851–858. (C) A. Zianna, G. Psomas, A. Hatzidimitriou, E. Coutouli-argyropoulou and M. Lalia-kantouri, *J. Inorg. Biochem*., 2013, **127**, 116–126. (d) C. Rajarajeswari, M. Ganeshpandian and M. Palaniandavar, *J. Inorg. Biochem*., 2014, **140**, 255–268.

14. (a) L. S. Kumar, K. S. Prasad and H. D. Revanasiddappa. *Chem. Eur. J*., 2011, **2**, 394–403; (b) A. Yan, T. Ming-Liang, J. Liang-Nian and M. Zong-Wan, *Dalton Trans*., 2006, 2066–2071.

15. Y. Lu, *Chem. Eur. J*., 2002, **8**, 4588–4596.

16. (a) M. J. Buckitt, *Methods Enzymol*., 1994, **234**, 66–79; (b) J. Hormann, C. Perera, N. Deibel, D. Lentz, B. Sarkar and N. Kulak, *Dalton Trans*., 2013, **42**, 4357–4360.

17. (a) J. Reedijk, *Chem. Commun*., 1996, 801–806; (b) W. Schmidt. and S. G. Chaney, *Cancer res*., 1993, **53**, 799-805F; (c) F. Arjmand and M. Muddassir, *Chirality*, 2011, **23**, 250–259; (d). R. Song, S. Y. Park, Y. S. Kim, Y. Kim, S-J. Kim, B. T. Ahn and Y. S. Sohn, *J. Inorg. Biochem*., 2003, **96**, 339–345; (e) D. M. Fisher, P. J. Bednarski, R. Grunert, P. Turner, R. R. Fenton and J. R. Aldrich-Wright, *ChemMedChem*., 2007, **2**, 488–495; (f) S. Kemp, PhD, *University of Western Sydney*, 2011; (g) M. L. Beetona, J. R. Aldrich-Wright and A. Bolhuis, *J. Inorg. Biochem*., 2014, **140**, 167–172; (h) J. F. Larrow and E. N. Jacobsen, *J. Org. Chem*., 1994, **59**, 1939-1942.

18. M.A. Linseis and D.G. Gilheany, *Tetrahedron:Asymmetry*, 2003, **14**, 2763–2769.

19. (a) P. Chandi, P. Kaliyamoorthy, C. Chung-Sun and L. L. Tian-Huey, *Polyhedron*, 1988, **17**, 2555–2561; (b) M. Roy, S. Dhar, B. Maity and A. R. Chakravarty. *Inorg. Chim. Acta*., 2011, **375**, 173–180.

20. K. Kamelia, K. Hamid and M. A. Hapipah, *Acta Crystallogr., Sect. E: Struct. Rep. Online*., 2011, **E67**, m421.

21. W. Xiao, S-R. Li, H. Zhou, Z-Q. Pana and Q. Huang. *Acta Crystallogr., Sect. E: Struct. Rep. Online*., 2011, **E67**, m701.

22. M. Jagadeesh, K. K. Suresh, L. S. Krishna and A. V. Reddy. *Spectrochim. Acta Part A*., 2014, **118**, 552–556.

23. (a) P. Kavitha and K. L. Reddy, *Arabian J. Chem*., 2012; (b) K. B. Guidance, S. A. Patil, R. S. Vadavi, V. S. Rashmi and M. S. Patil, *J. Serb. Chem. Soc*., 2006, **71**, 529–542.

24. A. H. Dawood, R. Khalaf and Z. Salman, *National. J. Chem.*, 2009, **35**, 489–505.

25. N. Raman, S. Ravichandran and C. Thangaraja, *J. Chem. Sci.*, 2004, **116**, 215–219.

26. T. M. Dunn, *The visible and ultraviolet spectra of complex compounds in modern coordination chemistry* (New York: Interscience) 1960.

27. F. Arjmand, G. C. Sharma, M. Muddassir and S. Tabassum, *Chirality*, 2011, **23**, 557–567.

28. (a) L. P. Battaglia, A. B. Corradi, L. Menabue and G. C. Pellacani, *J. C. S. Dalton*., 1981, 8–12; (b) V. M. Manikandamathavan and B. U. Nair. *Eur. J. Med. Chem*., 2013, **68**, 244–252.

29. A. K. Patra, M. Nethaji and A. R. Chakravarty, *J. Inorg. Biochem*., 2007, **101**, 233–244.

30. R. M. Patil and M. M. Prabhu, *Int. J. Chem. Sci*., 2010, **8**, 52–58.

31. W. E. Estes, D. P. Gavel, W. E. Hatfield and D. J. Hodgson, *Inorg. Chem*., 1978, **17**, 1415– 1421.

32. D. E. Nikles, M. J**.** Powers and F. L. Urbach, *Inorg. Chem*., 1983, **22**, 3210–3217.

33. O. I. Singh, M. Damayanti, N. R. Singh, R. K. H. Singh, M. Mohapatra and R.M. Kadam, *Polyhedron*, 2005, **24**, 909–916.

34. (a) K. P. Strotmeyer, I. O. Fritsky, R. Otta, H. Pritzkow and R. Kramer, *Supramol. Chem.*, 2003, 15, 529–547; (b) J. Chin, S. Chung and D. H. Kim, *J. Am. Chem. Soc*., 2002, **124**, 10948–10949.

35. Y. Zhao, J. Zhu, W. He, Z. Yang, Y. Zhu, Y. Li, J. zhang and Z. Guo, *Chem. Eur. J*., 2006, 12, 6621–6629.

36. (a) A. Barve, A. Kumbhar, M. Bhat, B. Joshi, R. Butcher, U. Sonawane and R. Joshi, *Inorg. Chem*. 2009, **48**, 9120–9132; (b) V. Rajendiran, R. Karthik, M. Palaniandavar, H. Stoeckli-Evans, V. S. Periasamy, Mohd. Abdulkader Akbarsha, B. S. Srinag and H. Krishnamurthy, *Inorg. Chem*., 2007, **46**, 8208−8221. (c) P. Kumar, S. Gorai, M. K. Santra, B. Mondal and D. Manna, *Dalton Trans.***,** 2012,**41**, 7573-7581.

37. (a) A. K. Patra, M. Nethaji and A. R. Chakravarty, *Dalt. Trans.*, 2005, 2798–2804; (b) A. Rajendran and B. U. Nair, Biochem. Biophys. Acta 2006, **1760**, 1794–1801.

38. R. Loganathan, S. Ramakrishnan, E. Suresh, A. Riyasdeen, M. A. Akbarsha and M. Palaniandavar, *Inorg. Chem.*, 2012, **51**, 5512−5532.

39. (a). S. Mahadevan and M. Palaniandavar, *Inorg. Chem.* 1998, **37**, 693–700; (b). A. B. Tossi and J. M. Kelly, *Photochem. Photobiol.* 1989, **9**, 545–556.

40. (a) H-H Luy, Y-T Li, Z-Y Wuz, K. Zhengy and C-W. Yan, *J. Coord. Chem*. 2011, **64**, 1360–1374 (b) T. M. Kelly, A. B. Tossi, D. J. McConnell and T. C. Strekas, *Nucleic Acids Res.* 1985, **13**, 6017–6037.

41. M. Murali, M. Palaniandavar and T. Pandiyan. *Inorg. Chim. Acta*., 1994, **224**, 19–25.

42. S. Mahadevan and M. Palaniandavar, Inorg. Chem. 1998, **37**, 693–700.

43. M.T. Carter and A.J. Bard. J. Am. Chem. Soc., 1987, **109**, 7528–7529.

44. (a) X. Pin-xian, X. Zhi-hong, C. Feng-juan, Z. Zheng-zhi and Z. Xiao-wen, *J. Inorg. Biochem*. 2009, **103**, 210–218; (b) L. Li, Q. Guo, D. Jianfang, X. Xu and J. Li, *J. Photochem. Photobiol., B*., 2013, **125**, 56–62; (c) E. Mrkali, A. Zianna, G. Psomas, M. Gdaniec, A. E. Czapik, E. C. Argyropoulou, L-K. Maria, *J. Inorg. Biochem*., 2014, **134**, 66–75; (d) M. Ganeshpandian, S. Ramakrishnan, M. Palaniandavar and E. Suresh, *J. Inorg. Biochem*., 2014, **140**, 202–212.

45. Z. Shouchun, X. Chun, Y. Chen and J. Zhou. *Chin. J. Chem*., 2011, **29**, 65–71.

46. E. Trotta, N. D. Grosso, M. Erba and M. Paci. *Biochem*., 2000, **39**, 6799–6808.

47. (a) V. Chandrasekhar, S. Tapas and R. Clérac, *Eur. J. Inorg. Chem*., 2009, 1640–1646; (b) S. Anbu, M. Kandaswamy, S. Kamalraj, J. Muthumarry and B. Varghese, *Dalton Trans*., 2011, **40**, 7310–7318; (c) S. S. Massoud, F. R. Louka, Wu Xu, R. S. Perkins, R. Vicente, J. H. Albering and F. A. Mautner, *Eur. J. Inorg. Chem*., 2011, 3469–3479; (d) D-D. Li, J-L. Tian, W. Gu, X. Liu and S-P. Yan, *Eur. J. Inorg. Chem*., 2009 5036–5045.

48. (a) D. S. Sigman, *Acc. Chem. Res*., 1986, **19**, 180–186; (b) J. E. Baiglow and A. V. Kachur, *Radiat. Res*., 1997, **48**, 181–187. (c) A.V. Kachur, Y. Manevich and J. E. Biaglow, *Free Rad. Res*., 1997, **26**, 399–408.

49. D. D. Perrin, W. L. Armarego and D. R. Perrin, *Purification of Laboratory Chemicals*, Pergamon, 2nd Edition New York, 1980.

50. Y. Gultneh, A. R. Khan, D. Blaise, S. Chaudhry, B. Ahvani, B. B. Marvey and R. J. Butcher, *J. Inorg. Biochem*., 1999, 75, 7–18.

51. P. Bhyrappa and P. Bhavana, *Chem. Phys*. *Lett*., 2002, **357**, 108–112.

52. C. P. Nash, *J. Phys. Chem*. 1960, **64**, 950–953.

53. A. Altomare, G. Cascarano, C. Giacovazzo and A. Guagliardi, *J. Appl. Crystallogr*., 1993, **26**, 343–350.

Mononuclear Zn(II) and Cu(II) Complexes with a Simple Diamine Ligand: Synthesis, Structure, Phosphodiester Binding and DNA Cleavage Studies

Popuri Sureshbabu[a] , A.A.J. Sudarga Tjakraatmadja[b] , Chittepu Hanmandlu[a], K. Elavarasan[a], Nora Kulak[b,*] and Shahulhameed Sabiah[a, *]

[a]Department of Chemistry, Pondicherry University, Pondicherry- 605 014, India.

[b]Institute of Chemistry and Biochemistry, Freie Universtität Berlin, Germany.

Graphical Abstract

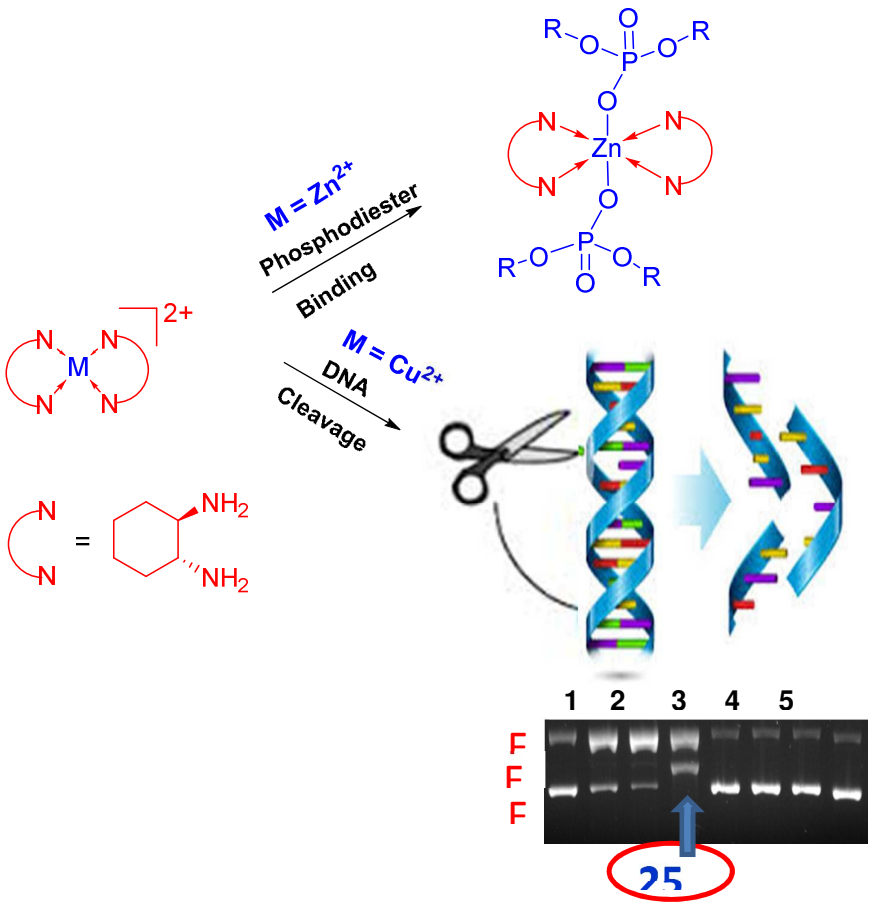

Graphical Synopsis

Mononuclear Copper(II) and Zinc(II) complexes with simple bidentate ligand (1,2-diaminocylohexane) were synthesized and characterized. They show binding affinity towards phosphodiesters (DPP, BNPP) and CT- DNA. Cu(II) complex with ascorbate as reductant efficiently cleaves supercoiled DNA up to Form III at 25 μM under oxidative pathway.